The formation and evolution of bars in low surface brightness galaxies with cold dark matter haloes

Mayer, Lucio ; Wadsley, James

Abstract: We perform several high-resolution simulations of low surface brightness galaxies (LSBGs) embedded in cold dark matter haloes to study how likely bar formation is in such systems. The behaviour of various collisionless galaxy models is studied both in isolation and in the presence of a large perturbing satellite. We also consider models with a dominant gaseous component in the disc. We find that in general bar formation requires disc masses at least a factor of 2 higher than those inferred for LSBGs under the assumption of a normal stellar mass-to-light ratio. Instead, if LSBGs have fairly light, low surface density discs, they are stable to the formation of a stellar bar within NFW (Navarro-Frenk-White) haloes spanning a range of concentrations. However, a purely gaseous light disc can form a bar for realistic temperatures provided that cooling is very efficient (we adopt an isothermal equation of state) and that the halo has a very low concentration, $c < 5$. The bars that form in these low surface brightness (LSB) models are significantly shorter than the typical halo scale radius — their overall angular momentum content might be too low to affect significantly the inner dark halo structure. Once formed, all the bars evolve into bulge-like structures in only a few gigayears and can excite spiral patterns in the surrounding disc component. The recently discovered red LSBGs show significant non-axisymmetric structure and bulge-like components, and share many of their structural properties with the final states of our LSB models with massive discs. Our results imply that a bulge-like component must be present in any LSBG that ever went bar-unstable in the past

DOI: https://doi.org/10.1111/j.1365-2966.2004.07202.x

Mon. Not. R. Astron. Soc. **347,** 277–294 (2004)

The formation and evolution of bars in low surface brightness galaxies with cold dark matter haloes

Lucio Mayer[1]★ and James Wadsley[2]

[1]*Institute for Theoretical Physics, University of Zurich, Winthethurestrasse 190, 8057 Zurich, Switzerland*
[2]*Department of Physics and Astronomy, McMaster University, 1280 Main St. West, Hamilton, Ontario L8S 4M1, Canada*

Accepted 2003 September 10. Received 2003 September 10; in original form 2003 March 11

ABSTRACT

We perform several high-resolution simulations of low surface brightness galaxies (LSBGs) embedded in cold dark matter haloes to study how likely bar formation is in such systems. The behaviour of various collisionless galaxy models is studied both in isolation and in the presence of a large perturbing satellite. We also consider models with a dominant gaseous component in the disc. We find that in general bar formation requires disc masses at least a factor of 2 higher than those inferred for LSBGs under the assumption of a normal stellar mass-to-light ratio. Instead, if LSBGs have fairly light, low surface density discs, they are stable to the formation of a stellar bar within NFW (Navarro–Frenk–White) haloes spanning a range of concentrations. However, a purely gaseous light disc can form a bar for realistic temperatures provided that cooling is very efficient (we adopt an isothermal equation of state) and that the halo has a very low concentration, $c < 5$. The bars that form in these low surface brightness (LSB) models are significantly shorter than the typical halo scale radius – their overall angular momentum content might be too low to affect significantly the inner dark halo structure. Once formed, all the bars evolve into bulge-like structures in only a few gigayears and can excite spiral patterns in the surrounding disc component. The recently discovered red LSBGs show significant non-axisymmetric structure and bulge-like components, and share many of their structural properties with the final states of our LSB models with massive discs. Our results imply that a bulge-like component must be present in any LSBG that ever went bar-unstable in the past.

Key words: hydrodynamics – methods: miscellaneous – methods: *N*-body simulations – galaxies: general – galaxies: interactions – galaxies: kinematics and dynamics.

1 INTRODUCTION

Deep surveys carried out in the past decade or so have unveiled a vast population of low surface brightness disc galaxies (LSBGs) that range from dwarf to fairly luminous galaxies and even giant spirals (Bothun, Impey & Malin 1986; Bothun et al. 1987; Schombert et al. 1992; Impey et al. 1996). Typical LSBGs are late-type objects characterized by blue colours, low metallicity, very high gas fractions and low levels of star formation activity. More recently, a new class of gas-rich, red late-type LSBGs has been discovered (O'Neil, Bothun & Schombert 2000), together with another population of red early-type LSBGs (Beijersbergen, de Blok & Van der Hulst 1999; Galaz et al. 2002). Some of the red LSBGs have metallicities close to the Solar value (Bergmann, Jorgensen & Hill 2003). Hence LSBGs probably span a range of properties comparable to 'normal' high surface brightness spiral galaxies (HSBGs). The high gas fractions of LSBGs suggest that they are quite unevolved objects with very low past and present star formation rates. The low metallicity (de Blok & Van der Hulst 1998a,b) and the low gas surface densities (de Blok, McGaugh & Van der Hulst 1996) can explain the low star formation rates of blue LSBGs (Gerritsen & de Blok 1999; Van den Hoek et al. 2000). The fact that LSBGs and HSBGs seem to follow the same Tully–Fisher relation (Zwaan et al. 1995; McGaugh et al. 2000) implies that the former have much higher dark matter contents than the latter within the region typically probed by the observations (of the order of a few disc scalelengths). This conclusion stems from the low stellar mass-to-light ratios suggested by the blue colours of most LSBGs, which imply that low surface brightness (LSB) really indicates low surface density (de Blok, McGaugh & Van der Hulst 1996b) – a higher dark matter density is then required to explain why these galaxies have circular velocities comparable to those of similarly luminous HSBGs (Verheijen & de Blok 1999). Hence LSBGs offer an ideal opportunity to study the distribution of dark matter and

★E-mail: lucio@physik.unizh.ch

to compare the observational results with current theories of structure formation. Predictions of cold dark matter (CDM) simulations were found to disagree with the rotation curves measured from H I emission in many dwarf galaxies and LSBGs (Moore 1994; Flores & Primack 1994).

Observed galaxies would have haloes with a constant density core, whereas simulated haloes have cuspy density profiles falling as r^{-1} (the NFW model, Navarro, Frenk & White 1997) or even steeper (Moore et al. 1999a). While some observers have pointed out several limitations of the original measurements of rotation curves based on H I emission from atomic hydrogen and have thus analysed several of the same galaxies using the stellar Hα line (Swaters, Madore & Trewhella 2000; Van den Bosch & Swaters 2001; Swaters et al. 2003), recent high-resolution data obtained using both techniques seem to confirm that the majority of the rotation curves of LSBGs cannot be fitted by the cuspy halo profiles predicted by CDM cosmogonies (de Blok, McGaugh & Rubin 2001a,b; de Blok et al. 2001c; de Blok & Bosma 2002). In dwarf galaxies, strong supernovae feedback might play a role in affecting the overall mass distribution (Navarro et al. 1996), but the quiescent star formation histories of LSBGs together with the fairly large potential wells of many of them rule out such a scenario (Bell et al. 1999; Bergmann et al. 2003).

Recently Weinberg & Katz (2002) have suggested that the dark matter cusp might be erased due to the dynamical interaction with a stellar bar. It has been known for a while that a rotating barred potential would slow down due to dynamical friction against the halo background, shedding its angular momentum to the latter (Hernquist & Weinberg 1992). Of course, the deceleration of the bar will be stronger in more massive haloes. Debattista & Sellwood (1998, 2000) were the first to note that the dynamical interaction between the bar and the halo could provide clues to the nature of the latter; they noted that, if galaxies have massive dark haloes as predicted by CDM models, it would be hard to explain why bars in many galaxies are quite fast rotators. On the other end, Valenzuela & Klypin (2003) claim that the net transfer of angular momentum to the bars is quite weak – bars slow down on a quite long time-scale even in CDM haloes as angular momentum is exchanged back from the halo to the individual stellar orbits supporting them once a sufficiently high force resolution is used in the simulations. Weinberg & Katz (2002) consider the idealized case of a very massive non-responsive bar and find that the resonant transfer of energy and angular momentum from the bar to an NFW halo can actually change the density profile of the latter, creating a constant density in only a few gigayears. The effect would occur only when the resonance structure of the halo is well resolved, which requires a very large number of particles in simulations, of the order of a few millions. Sellwood (2003), using a different numerical technique, finds the effect to be almost negligible for more realistic initial setups of the galaxies in which the bar is not imposed from the start and can evolve instead of being just a rigid potential. While further investigation of the effectiveness of the bar–halo interaction with self-consistent stellar bars is necessary, an even more basic question arises: Can this mechanism be at play in the most interesting case, namely that of LSBGs? How likely is it that these galaxies would go bar-unstable? Indeed, numerical studies on bar formation and bar–halo interactions have always employed models of high surface brightness galaxies. While bars seem to be ubiquitous among spiral galaxies as a whole (Eskridge et al. 2000), low surface brightness galaxies are expected to be stable to bar formation due to a combination of low disc self-gravity and high dark matter contents (Mihos, McGaugh & de Blok 1997). However, the current status of observations seems to suggest a quite complex scenario. In fact, while blue LSB disc galaxies are indeed typically non-barred (although some dwarf LSBGs have Magellanic bars), red LSBGs comprise several systems showing distortions, evident bars and even bulge-like components (Beijersbergen et al. 1999). Tidal encounters might also trigger bar formation or other non-axisymmetric distortions even in LSBGs (Mihos et al. 1997) and might actually be required to destabilize the gas in the discs and sustain star formation (Schombert, McGaugh & Eder 2001; Verde, Peng Oh & Jimenez 2002).

In this paper we study the formation of bars in models of LSBGs comprising a stellar and/or gaseous disc embedded in a dark matter halo whose structure is motivated by the results of CDM models. Such an approach is novel among studies of bar formation in galaxies, having been only partially adopted by Valenzuela & Klypin (2003). We have carried out a large set of high-resolution *N*-body/single-particle hydrodynamic (SPH) simulations using the parallel binary tree + SPH code PKDGRAV/GASOLINE (Stadel 2001; Stadel, Wadsley & Richardson 2002; Wadsley, Stadel & Quinn 2003).

Weinberg & Katz (2002) argue that, although present-day LSBGs might be stable to bar formation, they could have undergone a bar instability in the past when they first assembled a cold, massive disc. Although such a bar would have likely triggered a burst of star formation, this being difficult to reconcile with the many hints pointing towards a fairly smooth star formation history for these galaxies (Bergmann et al. 2003), observations still cannot exclude that at least the redder among these galaxies might hide a faded massive disc (O'Neil et al. 2000). Clearly the bulge-like components seen in many red LSBGs might be the result of secular evolution of an old bar (Combes & Sanders 1981; Carollo et al. 2001). In brief, the origin and nature of LSBGs is still subject to debate, and therefore we will consider a range of models covering a vast parameter space in terms of masses and internal structure of discs and haloes, the only two constraints being that the resulting rotation curves have to resemble those of observed LSBGs, i.e. they have to be slowly rising out to several disc scalelengths (de Blok & McGaugh 1997), and that discs have scalelengths bigger than those of HSBGs having the same luminosity (Zwaan et al. 1995).

Models with a major gaseous disc can represent either LSBGs during their early evolutionary stage or those numerous present-day LSBGs in which the baryonic mass is mostly contributed by the gas component (de Blok & McGaugh 1997). We note that the same disc model realized as purely gaseous instead of purely stellar is not expected to have the same stability properties. It has been shown that fluid configurations tend to be more stable because pressure is generally isotropic while the corresponding stellar analogue, the velocity dispersion, is generally anisotropic (Cazes & Tohline 2000). However, the study of the stability of purely gaseous discs embedded in dark matter haloes is new, to our knowledge. Works exist on the stability of generic axisymmetric or triaxial fluid configurations (Cazes & Tohline 2000; Barnes & Tohline 2001); on the stability of galactic discs with both a gaseous and a stellar component, and on how this depends on the numerical technique adopted (Romeo 1992, 1994); and even on bar-unstable exponential gaseous galactic discs (Friedli & Benz 1993, 1995) – but all these studies did not include any realistic dark matter component in their models and are therefore extremely idealized when applied to the dynamical evolution of real galaxies. The stability of gaseous and stellar systems, both uniformly rotating and differentially rotating, was also studied by Christodoulou, Shlosman & Tohline (1995) – these authors tried to extend to gaseous discs within dark haloes a criterion for stability against bar formation

originally developed by Efstathiou, Lake & Negroponte (1982) for stellar discs but did not test their conclusions with numerical simulations.

Finally, we will also consider the case of perturbations tidally induced by massive satellites, as expected during the hierarchical buildup of structures. Strong tidal interactions with even more massive galaxies would also occur in a hierarchical scenario and surely will drive bar formation but they would also transmute these fragile disc galaxies into spheroidals or even destroy them (Moore et al. 1999b; Mayer et al. 2001a,b).

The paper is organized as follows: in Section 2 we describe the models and the initial setup of the simulations, in Section 3 we illustrate the results of the simulations, Section 4 contains the discussion, and a summary follows in the last section.

2 GALAXY MODELS AND SIMULATIONS

Galaxy models are built as in Mayer et al. (2001b, 2002) using the technique originally developed by Hernquist (1993) (see also Springel & White 1999). We use a system of units such that $G = 1$, $[M] = 6.5 \times 10^9$ M$_\odot$ and $[R] = 6$ kpc. The models comprise a dark matter halo and an embedded stellar or gaseous disc (or both). Structural parameters were chosen in order to obtain slowly rising rotation curves resembling those published for LSBGs (e.g. de Blok et al. 2001a,b; de Blok & Bosma 2002; Van den Bosch & Swaters 2001). We start by choosing the value of the circular velocity of the halo at the virial radius, $V_{\rm vir}$, which, for an assumed cosmology (hereafter $\Omega_0 = 0.3$, $\Lambda = 0.7$, $H_0 = 65\,{\rm km\,s^{-1}\,Mpc^{-1}}$) automatically determines the virial mass, $M_{\rm vir}$, and virial radius, $R_{\rm vir}$, of the halo (Mo, Mao & White 1998). We choose $V_{\rm vir} = 75$ km s^{-1}, which corresponds to $M_{\rm vir} = 2 \times 10^{11}$ M$_\odot$ and $R_{\rm vir} = 120$ kpc. Haloes have NFW density profiles (Navarro, Frenk & White 1995; Navarro et al. 1997) with different halo concentrations, c, and spin parameters, λ (Mo et al. 1998). The concentration is defined as $c = R_{\rm vir}/r_{\rm s}$, where $r_{\rm s}$ is the halo scale radius; the spin parameter is defined as $\lambda = J\,|E|^{1/2} G^{-1}\,M_{\rm vir}^{-5/2}$, where J and E are, respectively, the total angular momentum and total energy of the halo and G is the gravitational constant.

The value of the concentration c basically defines what fraction of the total mass of the halo is contained within its inner regions, where the baryonic disc lies; the concentration increases with decreasing mass and, for a given mass, has a scatter of roughly a factor of 2, mainly due to different formation epochs (Bullock et al. 2001; Eke, Navarro & Steinmetz 2001). The average concentration for galaxies with $V_{\rm vir} \sim 75\,{\rm km\,s^{-1}}$ is $\sim$12 in the standard LCDM model assumed here. However, fitting rotation curves of LSBGs with NFW profiles often requires $c \lesssim 5$ (Van den Bosch & Swaters 2001; de Blok & Bosma 2002), at the lower end of the allowed range of values. We consider mainly three values for the halo concentration, $c = 4$, 7 and 12, but we also performed three runs with higher concentrations, $c =$ 16 and 22, to investigate further how bar formation can be affected by such parameter (these high concentrations are indeed more common than our lowest value, $c = 4$, for LCDM haloes at this mass scale).

Placing galaxy discs inside cosmological haloes would in principle require to have first solved the problem of galaxy formation in the LCDM scenario. Incidentally, whereas for years simulations of galaxy formation within CDM models have been plagued by the so-called angular momentum 'catastrophe' (Navarro & Steinmetz 2000), producing only tiny discs an order of magnitude smaller than those of real galaxies, new SPH simulations with considerably higher resolution and an improved treatment of gas dynamics find this problem to be significantly alleviated (Governato et al. 2002; see also Sommer-Larsen, Gotz & Portinari 2002; Thacker & Couchman 2001). These new simulations produce discs bearing scaling relations with their dark matter haloes reasonably close to the predictions of the semi-analytical models by Mo et al. (1998) – the latter are able to match the properties of spiral galaxies assuming angular momentum conservation of the baryons as they cool into the haloes and settle into a centrifugally supported disc (Fall & Efstathiou 1980). We thus construct models of LSBGs that follow the scaling relations of Mo et al. (1998). The procedure used to assign structural parameters is described in detail in Mayer et al. (2001b, 2002). Here we recall that we use exponential discs (with a few exceptions indicated below) and that their mass and scalelength are determined primarily by $M_{\rm vir}$ and λ and, to a minor extent, by the disc/halo mass ratio, $f_{\rm d}$, and halo concentration c (the latter two parameters contribute to specify the potential energy of the system and thus the rotational energy needed for centrifugal support). The adiabatic contraction of the halo in response to the accumulation of baryons at the centre is also taken into account (Springel & White 1999). As we mentioned in Section 1, the rotation curves of LSB disc galaxies suggest that these systems are extremely dark matter dominated, with stellar disc/halo ratios $\sim$0.03 or less, namely at least a factor of 2 lower than those of HSBGs of comparable luminosity (O'Neil et al. 2000; Chung, van Gorkom & O'Neil 2002). However, this difference probably reflects the fact that in LSBGs a larger fraction of the baryons, sometimes most of them, are found in the gaseous component; indeed, the total disc mass (stars plus gas) relative to the halo mass is quite similar in LSBGs and HSBGs (McGaugh et al. 2000). Previous works on the detailed mass modelling of LSBGs have indeed found a typical value of 0.065 for the total disc/halo mass ratio in these systems (Hernandez & Gilmore 1998).

We thus adopt the view that LSBGs are simply more extended than HSBGs because of larger halo spin parameters and eventually lower halo concentration, as originally suggested by Dalcanton, Spergel & Summers (1997) and Mo et al. (1998) (see also Jimenez et al. 1998; Hernandez & Gilmore 1998) and as confirmed more recently by Jimenez, Verde & Oh (2003) in their modelling of Hα rotation curves.

The disc mass fraction $f_{\rm d}$ is usually set equal to 0.05 or less in our models, but we also consider cases in which $f_{\rm d} = 0.1$, such a massive disc being expected in scenarios where LSBGs have a massive faded stellar component (O'Neil et al. 2000; Chung et al. 2002; Galaz et al. 2002). The highest value of $f_{\rm d}$ is still consistent with the upper limit set for $\Omega_{\rm b}$ by nucleosynthesis, $\sim$0.17 (Spergel et al. 2003). In this case, however, we are implicitly assuming that nearly all the baryons ended up in the disc (this is a somewhat extreme assumption – see Verde et al. 2002). Jimenez et al. (1998), who coupled a stellar population synthesis model to a simple galaxy formation scheme in the context of the hierarchical clustering, find that $\lambda > 0.05$ is required to match the surface brightness and colours of several 'blue' LSBGs. In our models, haloes have spin parameters either 0.065 or 0.1, larger than the mean value found in cosmological simulations, $\lambda \sim 0.04$ (e.g. Lemson & Kaufmann 1999; Gardner 2001) – these values yield a disc scalelength, $R_{\rm h}$, in the range 2–6 kpc, consistent with observations (e.g. Zwaan et al. 1995; O'Neil, Bothun & Schombert 1998). Although our haloes have $V_{\rm vir} \sim 75$ km s^{-1}, the different halo concentrations and the addition of the stellar disc produce a peak rotational velocity, $V_{\rm peak}$ (at $\sim 2R_{\rm h}$) between 95 and 130 km s^{-1}, within the range of the maximum rotation speeds measured for the majority of LSBGs in the samples by de Blok & McGaugh (1997) and de Blok & Bosma (2002). Indeed it is

only $V_{\rm peak}$ that is accessible to observations based on H I or Hα kinematics, not $V_{\rm vir}$, which is too far out in the halo. The rotation curves of the galaxy models are shown in Fig. 1.

The setup of the stellar disc is complete once the Toomre parameter, $Q(R)$, is defined (Toomre 1964). This corresponds to fixing the local radial velocity dispersion $\sigma_{\rm R}$, as $Q(R) = \sigma_{\rm R}\kappa/3.36G\Sigma_{\rm s}$, where κ is the local epicyclic frequency, G is the gravitational constant and $\Sigma_{\rm s}$ is the disc surface density. The velocity field of the disc is calculated as in Springel & White (1999, see also Hernquist 1993); in particular, the radial and vertical velocity dispersions are assumed to be equal, and the azimuthal velocity dispersion is determined from the radial dispersion using the epicyclic approximation. The Q parameter at $\sim$1 disc scalelength will be given as a reference; the latter is typically set equal to 1.2 (see Table 1 for the precise values adopted). Q, in combination with other parameters (Binney & Tremaine 1987; Mihos et al. 1997), determines the stability of the discs to bar formation. Examples of the initial profile of the Q parameter that characterizes the models can be found later in Fig. 4. Numerical studies done in the past suggest that $Q \gtrsim 2$ is needed for stability against stellar bar growth in isolated galaxies (Athanassoula & Sellwood 1986). However, these studies were conducted using galaxy models of 'normal' high surface brightness spiral galaxies, while our LSB models have a lower disc self-gravity and could well be stable even for smaller Q values (Mihos et al. 1997).

We note that models with $c = 4$–7, $\lambda = 0.065$ and $f_{\rm d} = 0.05$ have a central B-band surface brightness μ_{0B} between 22.5 and 23.5 mag arcsec^{-2} for a B-band stellar mass-to-light ratio $(M/L_B)_* = 2$. We avoid more extreme values of the surface density/brightness on purpose; indeed, our first objective is to investigate if the bar instability is possible at least among LSBGs at the bright end of the surface brightness distribution (de Blok & McGaugh 1997). The models with massive discs ($f_{\rm d} = 0.1$) would have a central surface brightness 0.5 mag lower than the threshold often used as a definition

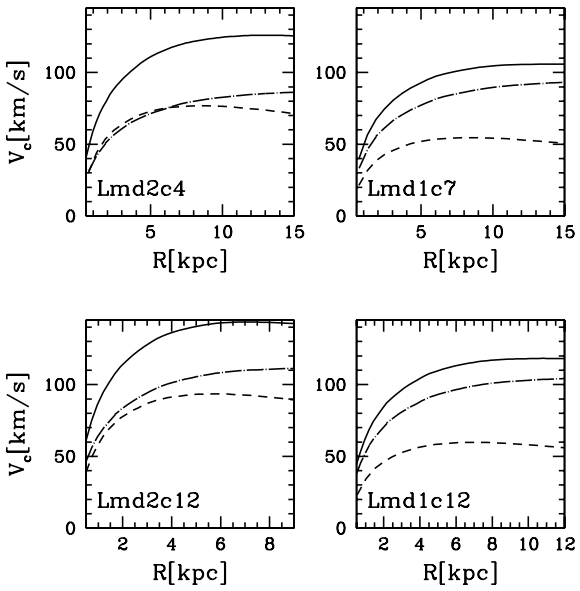

Figure 1. Rotation curves of galaxy models with purely stellar discs out to four disc scalelengths. The solid line denotes the total curve, while the dot-dashed and the dashed lines represent the separate contributions of, respectively, dark matter and stars. The name of each model is indicated in the panels (see Table 1).

Table 1. Parameters of the initial models. In models with both gas and stars, we indicate the parameters of only one component (the two components have identical structural properties in such models). The columns are described below the table.

Model (1)	$f_{\rm d}$ (2)	c (3)	λ (4)	$f_{\rm g}$ (5)	Gas profile (6)	$\varepsilon_{\rm d}$ (7)	Q (8)	X_2 (9)	$M_{\rm sat}/M_{\rm vir}$ (10)	Bar (11)	Bar length (12)
Lmd0c4	0.038	4	0.065	0	0	1.36	1.2	2.6	0	no	0
Lmd1c4	0.05	4	0.065	0	0	1.15	1.2	1.9	0	no	0
Lmd1c4Q2	0.05	4	0.065	0	0	1.15	1	1.9	0	no	0
Lmd1c4Q3	0.05	4	0.065	0	0	1.15	0.5	2	0	tr	0.6
Lmd1c7	0.05	7.5	0.065	0	0	1.18	1.2	2.42	0	no	0
Lmd1c12	0.05	12	0.065	0	0	1.28	1.2	2.47	0	no	0
Lmd2c4	0.1	4	0.065	0	0	0.703	1.2	1.36	0	yes	1.1
Lmd2c12	0.1	12	0.065	0	0	0.704	1.2	1.55	0	yes	1.6
Lmd2c12b	0.1	12	0.1	0	0	0.909	1.2	2.3	0	yes	2.1
Lmd2c16	0.1	16	0.065	0	0	0.86	1.2	1.75	0	yes	1.7
Lmd2c22	0.1	22	0.065	0	0	0.878	1.2	1.73	0	yes	2
Lmd2c22b	0.1	22	0.1	0	0	1.03	1.2	2.6	0	yes	1.8
Lmd1c4g	0.05	4	0.065	1	exp	1.15	1.2	1.9	0	yes	0.4
Lmd1c4gb	0.05	4	0.065	1	exp	1.15	1.5	1.9	0	no	0
Lmd2c4g	0.1	4	0.065	1	exp	0.703	1.2	1.36	0	yes	1.2
Lmd1c12g	0.05	12	0.065	1	exp	1.28	1.2	2.47	0	no	0
Lmd2c12g	0.1	12	0.065	1	exp	0.707	1.2	1.55	0	yes	1.9
Lmd1c4sg	0.05	4	0.065	0.5	exp	1.41	2.4	3.8	0	no	0
Lmd1c4gc	0.05	4	0.065	1	const.	1.4	2.2	10	0	no	0
Lmd1c12gc	0.05	12	0.065	1	const.	1.2	1.5	13	0	no	0
Lmd1c4sat	0.05	4	0.065	0	0	1.15	1.2	2	0.03	no	0
Lmd1c4Q3sat	0.05	4	0.065	0	0	1.15	0.5	2	0.03	tr	0.7
Lmd1c12sat	0.05	12	0.065	0	0	1.28	1.2	2.47	0.03	no	0

[a]Columns: (2) Disc/halo mass ratio. (3) Halo concentration. (4) Halo spin parameter. (5) Gas fraction. (6) Type of gas surface density profile. (7) Stability parameter. (8) Toomre parameter at one disc scalelength (note that models Lmd1c4gb and Lmd1c4g are identical except for the assumed gas temperature, hence the different resulting Q). (9) Parameter for swing amplification at one disc scalelength. (10) Mass of the satellite relative to total virial mass of the system. (11) Whether or not the system forms a bar ('tr' stands for transient). (12) Ratio between the maximum radius of the bar and the initial disc scalelength (the radius is found by directly measuring the extension of the bar in the density maps).

of LSBGs, $\mu_{0B} = 22.5$ mag arcsec^{-2}, for a stellar mass-to-light ratio $\sim$2, but, if representative of faded discs with $M/L_* \gtrsim 5$ (O'Neil et al. 2000), would have $\mu_b \geqslant 23.5$ mag arcsec^{-2}.

In the runs employing a gaseous disc, this has a temperature of 7500 K; the kinematics of the neutral hydrogen in the discs of spiral galaxies yield typical velocity dispersions consistent with this temperature (Martin & Kennicutt 2001). The gaseous disc has either a constant or an exponential surface density profile with the same scalelength of the disc (see Mayer et al. 2001b); in fact some LSBGs have rotation curves indicating that the H I component has a profile flatter than the stellar disc (e.g. de Blok & McGaugh 1997). In a gaseous disc the Toomre parameter is defined as $Q(R) = v_s\kappa/\pi G\Sigma_g$, where v_s is the sound speed and Σ_g is the surface density of the gas. For the assumed disc and halo masses, a temperature of 7500 K implies $Q \gtrsim 1$ throughout most of the galaxy, namely comparable to that of the collisionless runs. The Q profiles of two of the models are shown later in Fig. 5.

We do not include radiative cooling in the treatment of gas dynamics but we adopt an isothermal equation of state to model dissipation. This is somewhat idealized as it stands on the assumption that the thermal energy generated by, for example, shocks and supernovae explosions can be instantly radiated away, i.e. cooling is assumed to be very efficient. However, simulations of galaxy formation and evolution that explicitly include both radiative cooling and heating show that the temperature of the gas in galactic discs always stays close to 10^4 K (Hernquist & Katz 1989; Katz & Gunn 1991; Katz, Hernquist & Weinberg 1992; Gerritsen & Icke 1997; Navarro & Steinmetz 2000; Sommer-Larsen et al. 2002; Governato et al. 2002) – note however that lower temperatures are not allowed in many of these cited works because they usually adopt cooling functions with a cut-off at about 10^4 K. Supernovae might heat the gas very efficiently if the energy of their explosions is partly converted into turbulent motions (Thacker & Couchman 2001; Springel & Hernquist 2003) instead of being entirely converted into thermal energy, but their global impact on galaxies bigger than dwarfs is not yet established either observationally or theoretically (Martin 1999; MacLow & Ferrara 1999; Benson et al. 2003). We recall that the general expectation is that LSBGs should be quite stable to non-axisymmetric instabilities; in this context the assumption of an isothermal equation of state will provide the most favourable condition for the formation and survival of bars in gaseous discs by forcing the disc to remain cold (for instance, it might underestimate heating when a disc has already entered a phase of strong instability) – in reality the same systems can only be more stable if they retain some of the heat generated during their dynamical evolution.

However, in order to understand how sensitive the results are to the assumed equation of state, we evolve the same initial conditions with both an isothermal and an adiabatic equation of state (not shown in Table 1); the adiabatic runs represent the situation at the opposite extreme of the isothermal runs, namely radiative cooling is completely switched off.

A final type of model comprises systems in which the stellar and gaseous components make an equal contribution to the disc mass – this can reflect an evolutionary stage intermediate between those of models with purely gaseous and purely stellar discs. The rotation curves of some of the models with a gas component are shown in Fig. 2.

Gas dynamical simulations were carried out with GASOLINE, an extension of PKDGRAV (Stadel 2001), which uses SPH to solve the hydrodynamical equations (Stadel, Wadsley & Richardson 2002; Wadsley et al. 2003). The gas is treated as an ideal gas with equation of state $P = (\gamma - 1)\rho u$, where P is the pressure, ρ is the density, u is the (specific) thermal energy, and γ is the ratio of the specific heats (adiabatic index) which is set equal to 5/3 (we are assuming that the gaseous disc represents the atomic hydrogen component of the galaxy). In its general form the code solves an internal energy equation that includes an artificial viscosity term to model irreversible heating from shocks. The code adopts the standard Monaghan artificial viscosity as well as the Balsara criterion to reduce unwanted shear viscosity (Balsara 1995). In the isothermal case the thermal energy is constant over time and so no thermal energy equation is required (any heating resulting from the artificial viscosity term, which is still present in the momentum equation, is radiated away). In the adiabatic case the thermal energy can rise as a result of compressional and shock heating and can drop following decompressions.

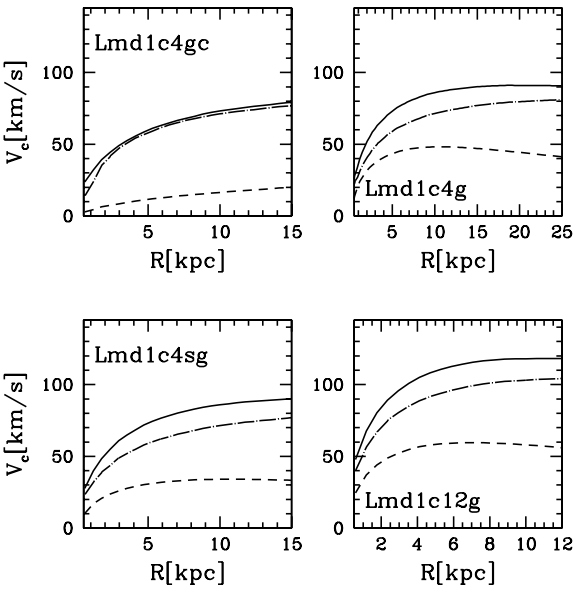

Figure 2. Rotation curves of galaxy models with a gaseous component out to four disc scalelengths. The solid line denotes the total curve, while the dot-dashed and the dashed lines represent the separate contributions of, respectively, dark matter and gas. The name of each model is indicated in the panels (see Table 1).

We also explore the case of LSBGs tidally disturbed by a massive companion having a mass comparable to that of the Large Magellanic Cloud (LMC). Other regimes of external tidal perturbations should not be relevant here. In fact, more massive satellites would rapidly merge at the centre before being substantially stripped (Colpi, Mayer & Governato 1999; Taffoni et al. 2003) and would likely destroy the fragile discs, while repeated fly-bys with even more massive galaxies in dense environments, like galaxy clusters or groups, would actually transform LSBGs into spheroidals or S0 systems (Moore et al. 1999b; Mayer et al. 2001a,b). For this set of runs we use LSBGs with purely stellar discs and the satellite is a deformable spherical halo with a fairly concentrated NFW profile ($c = 15$), a high concentration making the satellite stiffer and the associated perturbation stronger. The models used for these runs are indicated in Table 1. The satellite moves in the same direction as the disc rotation (prograde), which will maximize the tidal effects due to resonances between its orbital frequency and the frequencies of disc stars (Velazquez & White 1999). The orbital plane of the satellite coincides with the plane of the disc; this setup has been shown to be the most effective in triggering the formation of a bar by previous studies – the bisymmetric perturbing force acts during a longer time compared to when the companion orbit is inclined with

respect to the plane of the target (Gerin, Combes & Athanassoula 1990). We consider both a very eccentric (apo/peri = 15) and a nearly circular orbit (apo/peri = 2), both having a pericentre of 30 kpc, namely grazing the disc. Indeed, while repeated tidal shocks can be effective in driving global instabilities (Mayer et al. 2001b), near-resonant interactions between the satellite orbital frequency and the internal frequency of the galaxy might also excite strong non-axisymmetric modes in the disc (Gerin et al. 1990; Weinberg 2000; Weinberg & Katz 2002).

For the models with a single-component disc we use 500 000 or 1000 000 particles for the halo and 50 000 particles for the disc (either gaseous or stellar). In the models with a two-component disc we use 25 000 particles for both components and the same number of halo particles as before. In order to test how our results depend on resolution, we also performed runs in which the latter is doubled or tripled in either the dark or the baryonic component. Throughout the paper the results of the collisionless runs with 1000 000 particle haloes are shown, while gas dynamical runs have 500 000 particle haloes (the latter are generally more computationally expensive, hence the choice of a lower resolution). The resolution used for the halo is more than adequate to study physical bar formation – previous work showed that, with a few hundred thousand particles in the halo, spurious bar modes cannot be triggered in otherwise stable galaxies (Mayer et al. 2001b).

The only other existing work in which N-body simulations of bar formation with similarly high resolution were performed is Valenzuela & Klypin (2003); compared to them we use a lower force resolution, i.e. we employ a (spline) gravitational softening corresponding to 0.05 $R_{\rm h}$ (for both the stars and the gas) while they use $0.01R_{\rm h}$. However, a small softening is not necessarily a good choice – force resolution must be balanced with mass resolution in order to avoid increasing the noise due to the discrete representation of the systems (Hernquist, Hut & Makino 1993; Moore, Katz & Lake 1996) and our conservative choice has been widely tested in this respect (Mayer et al. 2001b). Yet the softening adopted is smaller than the smallest among the physical scalelengths present in the simulations, i.e. the disc scaleheight h, $h \sim 0.1R_{\rm h}$, which ensures that the stability properties of the galaxy models are not artificially enhanced (Romeo 1992, 1994).

Yet, in order to test how the results depend on force resolution, we have also run selected models a second time using the same softening as in Valenzuela & Klypin (2003), without finding any significant differences in the results.

3 RESULTS

We evolve the various initial galaxy configurations for up to 10 Gyr, which corresponds to several disc dynamical times (this being of the order of a few times 10^8 yr) and represents a significant fraction of the cosmic time. The developing of non-axisymmetric structure in our galaxy models can be seen in the projected colour-coded density maps shown in this section. We also quantify the strength of such distortions by means of the ellipticity parameter $\epsilon = 1 - b/a$, where a and b are the major and intermediate axis of the baryonic component of the galaxies (measured on the basis of the principal mass moments; $\epsilon = 0$ if the galaxy is axisymmetric). The ellipticity has been found to be a good measure of the strength of bars in a large number of studies as it correlates with more physical parameters like the ratio between the radial and axisymmetric components of the force (Martin 1995; Regan & Elmegreen 1997; Laurikainen, Salo & Rautiainen 2002; Laurikainen & Salo 2002). Although both bar mass and ellipticity would be needed to fully specify the bar contribution to the overall stellar potential of the galaxy, the latter is the only parameter easily accessible by the observations (Martin 1995).

3.1 Collisionless runs

LSB models with either low or high concentration and $f_{\rm d} < 0.1$ do not undergo any bar instability if $Q > 1$ (taking Q at roughly 1 disc scalelength as a reference – see Table 1). The stability of these models should be even more robust at higher resolution as numerical noise is suppressed and spurious non-axisymmetric modes induced by the discrete representation of the collisionless fluid are reduced (Hernquist 1993). A transient bar appears after 3–4 Gyr in LSB models with $c = 4$ haloes and $f_{\rm d} = 0.05$ only when Q is as low as 0.5 (see Table 1).

The bar scalelength is small, roughly $0.5R_{\rm h}$ (see Table 1). The results for such 'light' disc models can be found in Figs 3, 4 and 6. Instead, models with massive discs, $f_{\rm d} = 0.1$, become bar-unstable regardless of halo concentration and the value of Q. We emphasize that these massive discs form a bar even in models Lmd2c22a,b (see Table 1), which have the highest concentration ($c = 22$). With such high disc masses, bars are strong (the ellipticity of the stellar component in the bar region can be as high as 0.8) and long-lived (bottom panel of Figs 3 and 12). Bars form rapidly, after about 2 Gyr, of the order of a few disc dynamical times at $R = R_{\rm h}$, and reach out to $\sim 1R_{\rm h}$ in low-concentration haloes, and are longer, ~ 1.5–$2R_{\rm h}$, in high-concentration haloes. The maximum lengths of bars estimated from the density maps for the different models are listed in Table 1 (note that similar bar lengths are obtained if we calculate the mass moments and we define the bar to be the region of the galaxy with an ellipticity $\geqslant 0.7$). We tested that our results are not compromised by numerical effects, especially two-body scattering between stellar particles and more massive halo particles (Moore et al. 1996) and lack of force resolution that might bias the evolution of the galaxy potential (Dehnen 2001). We did this by (a) comparing runs with 500 000 particle haloes with runs having 1000 000 particle haloes and (b) comparing 1000 000 particle runs with a force resolution five times higher than the standard one (i.e. employing a softening five times smaller) in both the dark matter and the stellar component. The formation of the bar rearranges considerably both the kinematics and the surface density of the galaxies (see Section 3.3 for the subsequent morphological evolution of the bars), and this is reflected in the strong variations of the Q profiles, which change considerably less in the stable models (Fig. 4).

At higher values of the halo concentration, a higher shear is present near the centre and swing amplification of $m = 2$ modes is expected to be weak unless Q is extremely low (Binney & Tremaine 1987).

The susceptibility of a differentially rotating thin disc to swing amplification of some particular mode m can be measured by the parameter $X_m = R\,\kappa^2/2\pi m G\Sigma$ (Toomre 1981). For $m = 2$ modes, $X_2 < 3$ is required for strong swing amplification in potentials associated with flat rotation curves (Binney & Tremaine 1987), but a lower threshold, $X_2 < 2$, has been found for systems with slowly rising rotation curves such as those of our LSB models (Mihos et al. 1997; Mayer et al. 2001b). The X_2 parameter at $R = R_{\rm h}$ is always higher for haloes with higher concentration for a given value of $f_{\rm d}$ (see Table 1). A higher susceptibility to swing amplification might explain why, among light disc models that do not form a bar, a more pronounced non-axisymmetry arises in the ones with a lower concentration (Fig. 6). On the other hand, X_2 is within the regime of expected strong swing amplification only for the models with

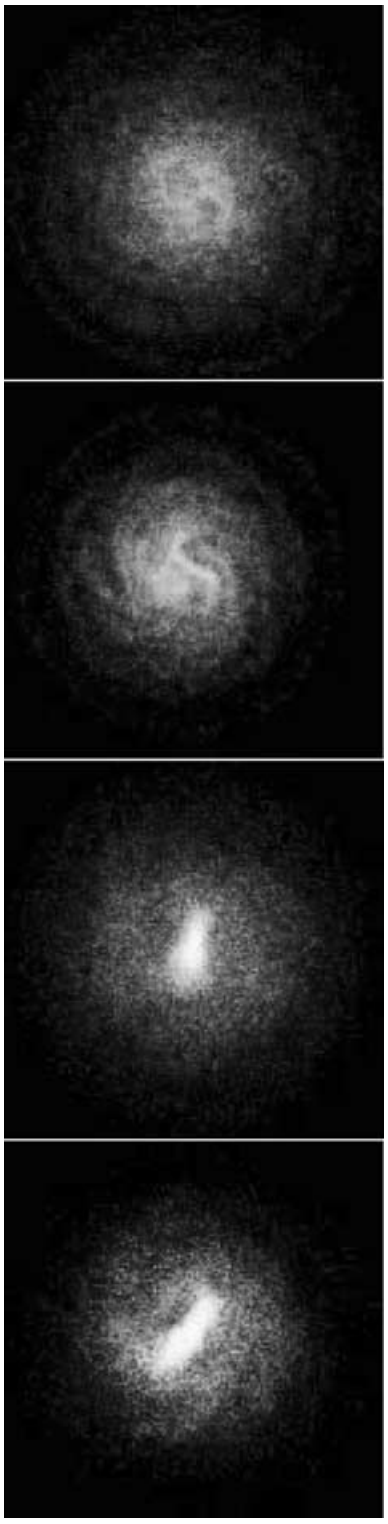

Figure 3. Grey-scale face-on view of the stellar density after 3 Gyr of evolution for some of the collisionless galaxy models (see Table 1). From top to bottom: Lmd1c4, Lmd1c4Q3, Lmd2c4 and Lmd2c12. Brighter shades correspond to higher densities; a central bar is evident in some cases. Boxes are 20 kpc on a side. This figure is available in colour in the on-line version of the journal on *Synergy*.

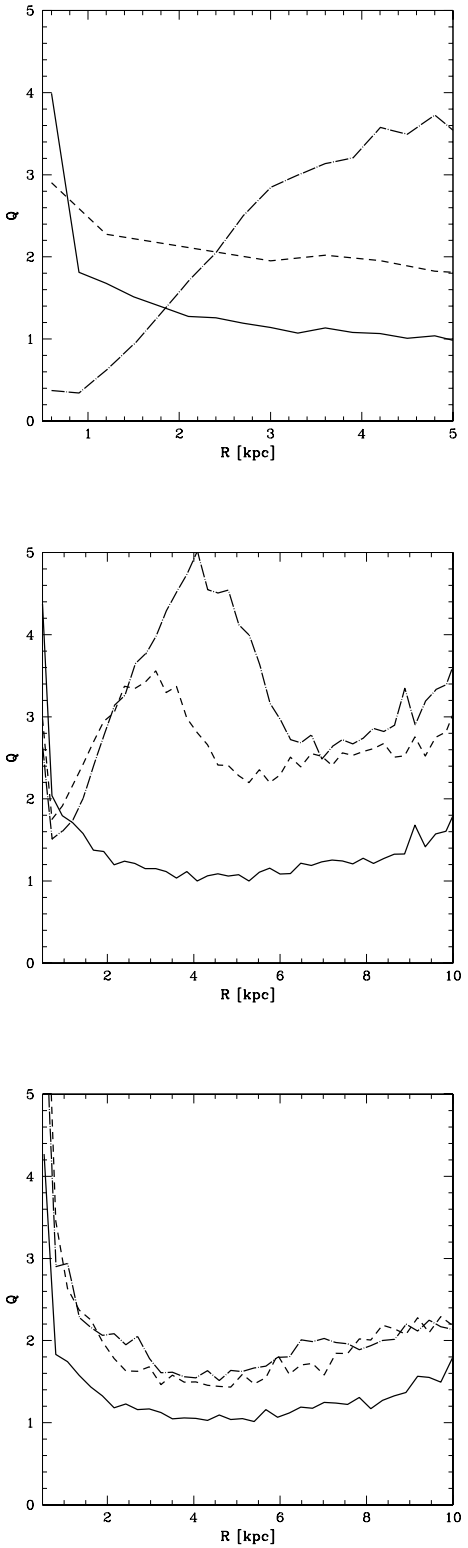

Figure 4. Evolution of the Q profile for three of our collisionless runs. The profiles at $t = 0$ (solid line), $t = 2.5$ Gyr (dashed line) and $t = 5$ Gyr (dot-dashed line) are shown, for model Lmd2c4 (top), model Lmd2c12 (middle) and model Lmd1c4 (bottom). The first two models form a bar (after 2 and 1.5 Gyr, respectively), while the third one is stable to bar formation (see Table 1).

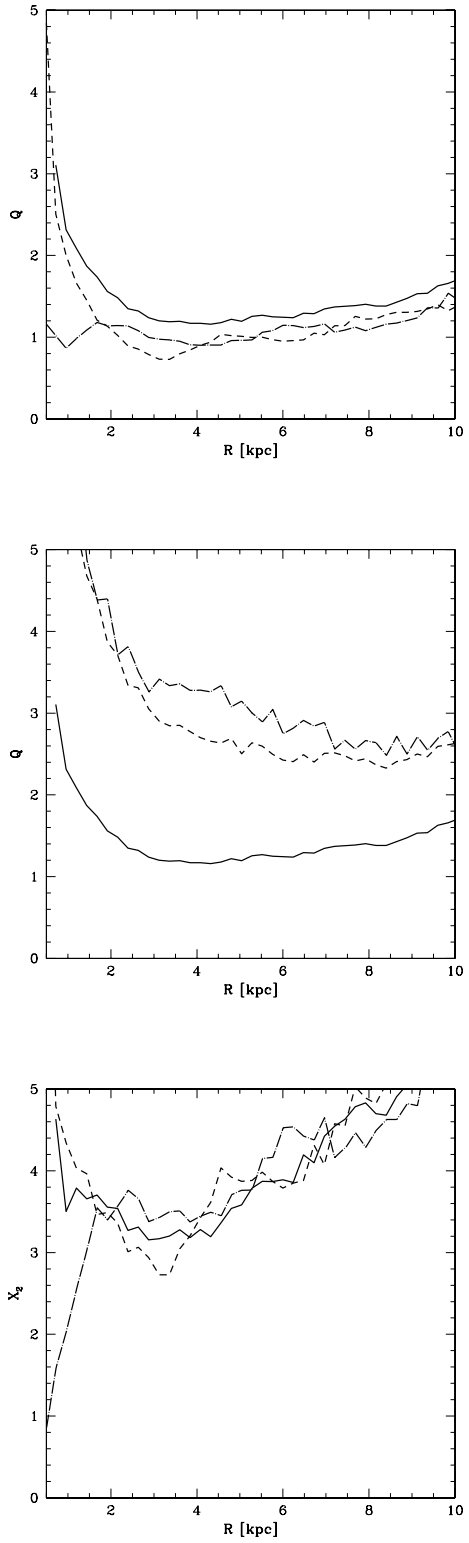

Figure 5. Evolution of the Q profile for two of our gas dynamical runs. The profiles at $t = 0$ (solid line), $t = 2.5$ Gyr (dashed line) and $t = 5$ Gyr (dot-dashed line) are shown, for the isothermal (top) and the adiabatic (middle) run with model Lmd2c12 (see Table 1). The isothermal model becomes bar-unstable slightly after $t = 5$ Gyr; for this simulation we also show the evolution of the X_2 parameter (bottom panel) – this indicates that at $t = 5$ Gyr strong swing amplification becomes possible within the inner 2 kpc.

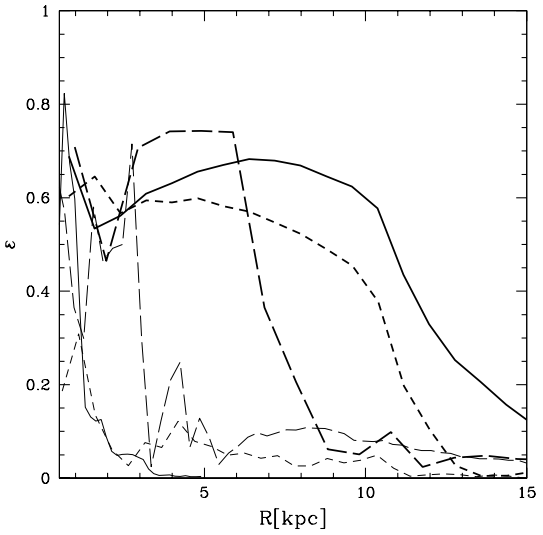

Figure 6. Ellipticity parameter of the stellar component in some of the collisionless simulations after 3 Gyr of evolution. The ellipticity is measured in concentric radial bins. The thick solid line is for model Lmd2c12, the thick short-dashed line for model Lmd2c4, the thin short-dashed line for model Lmd1c7, the thick long-dashed line for model Lmd1c4Q3, the thin solid line for model Lmd1c12 and the thin long-dashed line for model Lmd1c4. In barred systems (e.g. model Lmd2c4), the mass distribution remains significantly non-axisymmetric even outside the bar region.

$f_{\rm d} = 0.1$ (for these the values of X_2 are also very similar). The latter models are also those in which a bar always forms. We recall that X_2 depends on both halo concentration and disc mass through the ratio $\kappa^2/\Sigma_{\rm d}$. It can be shown (Mo et al. 1998; Springel & White 1999) that a more concentrated halo harbours a smaller disc (at fixed disc mass), the trend being even stronger with the inclusion of the adiabatic contraction, and therefore the changes in κ and $\Sigma_{\rm d}$ tend to compensate, yielding a nearly constant X_2. In brief, in our simulations the disc mass fraction is definitely more important than the concentration in setting both the degree of swing amplification and the development of the bar instability. Once initiated, swing amplification cannot proceed if a strong Lindblad inner resonance is present that cuts off the feedback cycle (Binney & Tremaine 1987; Sellwood & Evans 2001). This can be another way by which galaxies can avoid developing a bar. We checked the height of the Lindblad barrier for different models. We conclude that stellar frequencies that can be swing amplified always lie above the inner Lindblad resonance and hence this mechanism is negligible in our simulations, although the barrier is certainly higher when a high-concentration halo is present.

We find that the $\varepsilon_{\rm d}$ parameter introduced by Efstathiou et al. (1982) provides a good measure of the stability against bar formation. This parameter is defined as $\varepsilon_{\rm d} = V_{\rm peak}/\sqrt{(GM_{\rm d}/R_{\rm h})}$, where $V_{\rm peak}$ (see Section 2) is proportional to the mass of the dark halo within about one disc scalelength, and the denominator is proportional to the disc self-gravity ($M_{\rm d}$ is the disc mass). In Table 1 we list the values of $\varepsilon_{\rm d}$ for the galaxy models and we indicate whether the galaxy model is found to be stable or unstable to bar formation. In Efstathiou et al. (1982) it was found that $\varepsilon_{\rm d} \gtrsim 1.1$ was required for stability against bar formation; we find a very similar threshold, $\varepsilon_{\rm d} \gtrsim 1$. The fact that $\varepsilon_{\rm d}$ does not account for several dynamical aspects of bar formation, like the stabilizing effect of a large velocity dispersion of the disc and the possible interruption of swing amplification by the Lindblad barriers, and yet it provides a reasonable

fit to our results, strengthens our interpretation that the halo/disc mass ratio within the typical disc radius, which is related to both halo concentration and disc mass fraction (see rotation curves in Figs 1 and 2) is really the main factor determining the behaviour of our galaxy models [had we included models with 'hard centres' produced by, for example, bulges, the incompleteness of this criterion would have been more manifest (see Sellwood & Evans 2001)]. Even so, $\varepsilon_{\rm d}$ alone provides only a sufficient condition for stability to bar formation; a necessary and sufficient condition (at least for the present models) can only be obtained by coupling it with another parameter, for instance Q, and this is shown by comparison between models Lmd1c4, Lmd1c4Q2 and Lmd1c4Q3 – for the same $\varepsilon_{\rm d}$, a (transient) instability happens only when $Q < 1$ (see Table 1 and Fig. 3).

Galaxy models with highly concentrated haloes are stable even when satellites perturb them during several close passages over 10 Gyr (model Lmd1c12sat, see Fig. 8). Models with low-concentration haloes undergo a bar instability only if the disc has the lowest value of Q (Lmd1c4Q3sat) but this is weak and transient exactly as in the case where the galaxy is isolated, and the galaxy only shows mild non-axisymmetric distortions after several gigayears (Fig. 8). We find these conclusions to hold regardless of whether the orbit of the satellite is nearly circular or nearly radial. On a very eccentric orbit the impulsive heating at pericentre drives the formation of outer spiral arms in the disc. Therefore, the perturbing satellite does not appear to trigger the bar instability in the discs: this is in contrast to what is observed when an LSB satellite interacts with a much more massive galaxy halo (Mayer et al. 2001a,b), suggesting that only extremely strong perturbations can stimulate the growth of bar modes in these low surface density discs. In conclusion, in order to grow bars, models need a baryonic fraction as high as 10 per cent of the total mass for a spin parameter $\sim$0.065. This is more than a factor of 2 higher than the baryon fraction estimated for most observed LSBGs (Hernandez & Gilmore 1998). Of course, one could imagine that current surveys are still missing a fraction of the baryons of LSBGs because these galaxies are very extended and/or have a significant old stellar population not detectable in the optical (O'Neil et al. 2000; Galaz et al. 2002). Even so, the required baryon content is quite high, being close to $\gtrsim$0.13, the upper limit indicated by nucleosynthesis (Fukugita, Hogan & Peebles 1998) – but note that the new *WMAP* data allow for a sensibly higher upper limit, $\sim$0.17 (Spergel et al. 2003). Hence the models with massive discs are somewhat extreme as they demand that more than 50 per cent of the baryons available to the galaxy have already cooled into the disc. As mentioned in Section 2, if $(M/L_B)_* = 2$, model Lmd2c12g has a surface brightness high enough to be close to the upper limit usually adopted as a definition of an LSB galaxy in surveys ($\mu_B \sim 22.5$ mag arcsec^{-2}), while it would be a more typical LSB when placed in a low-concentration halo ($\mu_B \sim 23.5$ mag arcsec^{-2}); this is because in our modelling more concentrated haloes naturally produce more compact discs (Mo et al. 1998). One option to bring down the initial surface density/brightness (keeping $V_{\rm vir}$ and $f_{\rm d}$ fixed) is to start from a larger value of the spin parameter, which would reduce the disc surface density by spreading the same disc mass over a larger radius. To explore the latter hypothesis we simulated a galaxy with $\lambda = 0.1$ and $c = 12$ (model Lmd2c12b, see Table 1) that would have a lower surface brightness (>23.5 mag arcsec^2), which is more 'average' for LSBGs. Such a model still goes bar-unstable after $\sim$2.5 Gyr. Analogous results are also obtained running another high-spin model with even higher concentration (Lmd2c22b, see Table 1), although this would have a slightly higher surface brightness (by about 0.6 mag). Hence there is some flexibility in the choice of the disc surface density that can lead to bar formation, even for a highly concentrated halo, but always provided that the disc is sufficiently massive.

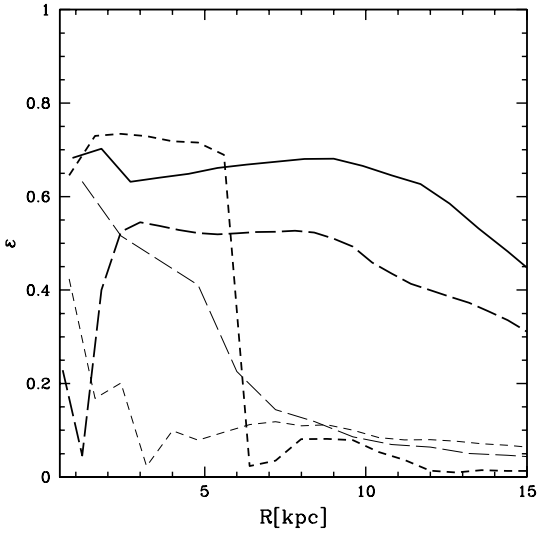

Figure 7. Ellipticity parameter of the gaseous component in gas dynamical runs. The ellipticity is measured in concentric radial bins. Models Lmd2c12g (thick solid line for the isothermal simulation and thick long-dashed line for the adiabatic simulation), Lmd1c4g (thick short-dashed line for the isothermal simulation and thin short-dashed line for the adiabatic simulation) and Lmd2c4sg (thin long-dashed line) are shown after, respectively, 3, 5 and 3 Gyr (i.e. at the time where the strongest non-axisymmetry is apparent in their density maps). Note that that in barred systems (e.g. Lmd2c12g) the galaxy is significantly non-axisymmetric ($\varepsilon \sim 0.5$) even outside the bar due to the presence of spiral patterns.

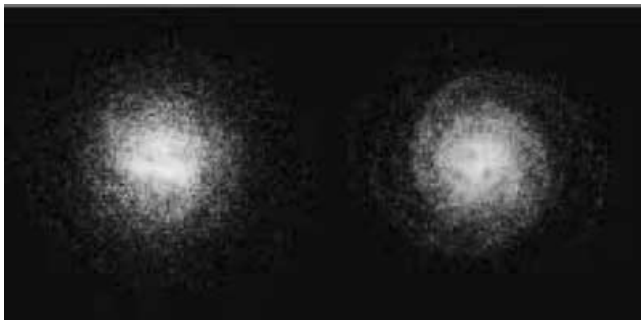

Figure 8. Grey-scaled face-on view of the stellar density of model Lmd1c12 (left) and Lmd1c4Q3 (right) perturbed by a satellite on a prograde orbit with, respectively, apo/peri = 2 and apo/peri = 15 (see text). Brighter shades represent higher densities. Snapshots are taken after 6 Gyr, when the satellite has performed roughly three orbits. Boxes are 30 kpc on a side. This figure is available in colour in the on-line version of the journal on *Synergy*.

3.2 Gas dynamical runs

The simulations employing an exponential gaseous disc with $f_{\rm d} = 0.05$ and an isothermal equation of state show results that are noticeably different from those of the corresponding collisionless runs. A distinct bar forms within a $c = 4$ halo (Lmd1c4g, see Fig. 9) after 5 Gyr, while only a short-lived bar-like distortion was observed in the corresponding collisionless run and only for the lowest initial value of Q (model Lmd1c4Q3, see Table 1). Only milder non-axisymmetric patterns, either spiral-like or oval, appear after

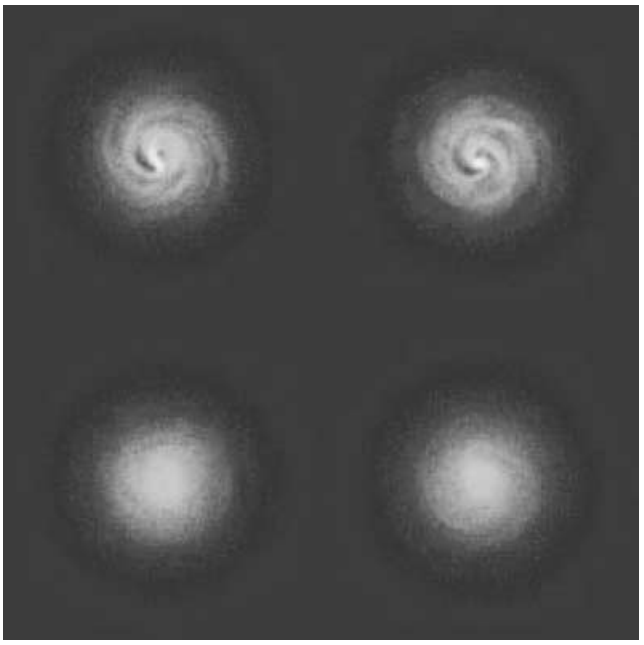

Figure 9. Grey-scaled face-on view of the gas density in model Lmd1c4g. Brighter shades represent higher densities. From the upper left to the bottom right, snapshots are shown at 5 and 8 Gyr for, respectively, the isothermal run and the adiabatic run. Boxes are 30 kpc on a side. This figure is available in colour in the on-line version of the journal on *Synergy*.

a few gigayears in haloes having $c = 12$ (Lmd1c12g). Later these patterns evolve into clump-like structures near the peaks of the surface density distortions. We note that the bar that forms in Lmd1c4g is visibly shorter than that produced in any of the stellar dynamical models (its radius is $\sim 0.3R_{\rm h}$). Once formed, the bar quickly evolves (in 1–2 Gyr, of the order of its rotation period) into something resembling an oval distortion and then a bulge-like component (Fig. 9). It is thus a really short-lived feature during the evolution of the gaseous disc. Raising the initial disc temperature by about 50 per cent (model Lmd1c4gb in Table 1) is enough to prevent the growth of the bar. None the less, this simulation suggests that cold gaseous discs appear more prone to undergoing non-axisymmetric instabilities with respect to their stellar analogue (see also Fig. 7 on the ellipticity). The reason is that the temperature is constant with time for model Lmd1c4g, while its stellar dynamical analogue, the velocity dispersion, is not constant in the corresponding collisionless models (e.g. Lmd1c4); instead it actually increases with time, driving Q towards large values. After 4 Gyr (just before the bar appears in model Lmd1c4g) the average velocity dispersion of model Lmd1c4 has increased by a factor of 2.5 within the disc scalelength in response to weak spiral instabilities, and Q close to or higher than 2 results throughout the disc, too high for the bar to develop (Fig. 4).

We tested whether the gaseous disc would respond in a similar way if cooling was inefficient; we thus evolved the same disc adiabatically for 6 Gyr and we found that, as expected, no bar forms in this case. In fact, after 4 Gyr, the temperature has grown by more than a factor of 5 in the inner few kiloparsecs (reaching 35 000 K), which raises Q by about a factor of 2 ($Q \propto T^{1/2}$). The disc now looks even smoother than the stellar disc, i.e. even less non-axisymmetric structure is present (compare Figs 9 and 3 and the measures of the ellipticities in Figs 6 and 7). The remarkable difference in the evolution of the Q profile of model Lmd1c4g in the isothermal and adiabatic runs can be appreciated in Fig. 5. Note that, within a few kiloparsecs from the centre, Q actually decreases slightly with time in the isothermal run, probably as a result of mass inflow from non-axisymmetric torques (which raise the disc surface density). In addition, the X_2 parameter, which initially is above the threshold for swing amplification (see Table 1), decreases even more, and in particular falls below the threshold for stability after about 4 Gyr, which corresponds to the time at which the bar first appears in the central region (bottom panel in Fig. 5). It is tempting to relate the small size of the bar to the tiny region of expected strong swing amplification, and this will be explored in a forthcoming paper, where we will investigate in more detail the nature of gaseous bars (Mayer, Debattista & Wadsley, in preparation). However, the isothermal calculations are probably more realistic at least in a global sense as cooling should be efficient enough to keep the temperature of the H I disc below 10 000 K (Martin & Kennicutt 2001 – see also Section 2). Therefore, we tend to conclude that in reality gaseous discs should be more susceptible to growing bars compared to stellar discs, although this does not imply anything about the relative longevity of the two types of bars (see below).

The disc evolution is also dependent on the type of gas profile. In models where the gaseous disc has a constant gas density profile (and is evolved isothermally), a strong bar does not appear in either low- or high-concentration haloes. In these models the surface density of the gaseous disc is too low everywhere (see the rotation curves in Fig. 2 and the values of the stability parameters in Table 1 – $\varepsilon_{\rm d}$ is computed using the disc half-mass radius in place of the scalelength used for exponential discs) and therefore it is not surprising that the growth of bar modes is suppressed.

Massive gaseous discs ($f_{\rm d} = 0.1$, models Lmd2c12g or Lmd2c4g) become strongly bar-unstable in a similar fashion as their stellar counterparts (Fig. 10). The bar instability appears even when the same models are evolved using an adiabatic equation of state. The instability in massive gaseous discs is 'dynamical' as in the collisionless case – it arises early, on a time-scale comparable to the

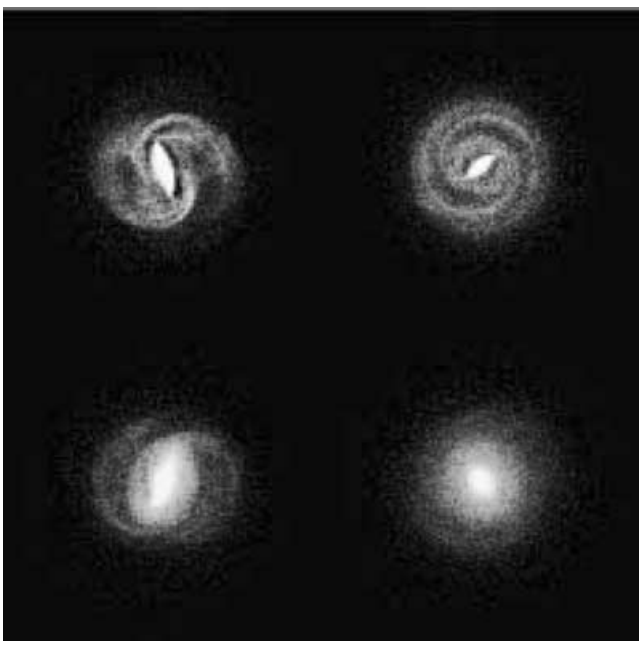

Figure 10. Grey-scaled face-on view of the gas density of model Lmd2c12g. Brighter shades represent higher densities. From the upper left to the bottom right, snapshots are shown at 3 and 6 Gyr for, respectively, the isothermal run and the adiabatic run. Boxes are 30 kpc on a side. This figure is available in colour in the on-line version of the journal on *Synergy*.

dynamical time of the disc (Fig. 10). The bar morphology evolves faster than in the stellar dynamical case, resembling more an oval distortion after a few bar rotations (one rotation period being about 4 Myr), as shown in Fig. 8. This difficulty shown by the gaseous discs in sustaining a barred potential was also reported by Friedli & Benz (1993), who found that the periodic x_1 orbits that support a stellar bar are quickly destabilized by shocks developing in their loops. Shocks are indeed clearly visible along the bar edges in our gas dynamical runs and the elongation of the density distribution decreases rapidly, especially in the adiabatic runs, where a higher pressure develops that smears out the density perturbation.

Christodoulou et al. (1995) have extended the stability criterion based on $\varepsilon_{\rm d}$ to gaseous discs within haloes, deriving $\varepsilon_{\rm d} \gtrsim 0.9$ as a condition for stability to bar formation in the latter systems. Their result was not based on numerical simulations of disc plus halo systems but was obtained from a comparison between quite idealized ellipsoidal fluid configurations and their stellar analogues. Our numerical results confirm that gaseous models are slightly more stable than stellar discs if we compare models starting with a similar initial Q and $\varepsilon_{\rm d}$ and there is no cooling (as in the adiabatic case), However, in general $\varepsilon_{\rm d} \gtrsim 1.2$ for stability, i.e. we obtain a criterion slightly stronger than for stellar discs if we take into account the effect of cooling (isothermal case). With efficient cooling, gaseous bars appear to weaken sooner than stellar bars, as suggested by the faster rounding of the central stellar density, and the reason is quite certainly the larger amount of mass transfer towards the central region (compare Figs 16 and 17 below).

In the model where stars and gas contribute equally to the disc (model Lmd1c4gs), each of the two baryonic components has a surface density reduced by 50 per cent compared to the corresponding models with a single baryonic component (Lmd1c4 or Lmd1c4g) and a bar does not form (Fig. 11). Analytical calculations and numerical experiments have shown that a disc made of stars and gas can be more susceptible to gravitational instability than either of its individual components would be (Jog 1992; 1996; Elmegreen 1995). However, those results apply when at least one of the components is marginally unstable (yielding $Q \sim 1$), whereas in the present case the surface density is very low for both components and, as a consequence, all the relevant parameters have values well within the regime of stability (see Table 1).

3.3 Morphological evolution of the bars

In models that go bar-unstable (both stellar and gaseous), we always observe a morphological evolution from a bar into a bulge-like central structure over a few bar dynamical times (a few gigayears, see Figs 10, 12 and 13), in agreement with the secular evolution scenario (Combes & Sanders 1981; Combes et al. 1990; Merritt & Sellwood 1994; Carollo et al. 2001). In the latter, vertical instabilities occur locally as a consequence of resonances between the bar rotation speed and the vertical oscillation frequency of the stars (Combes & Sanders 1981) or simply result because the orbital families supporting a flat, radially anisotropic bar become unstable to bending modes (Pfenniger 1984, 1985; Raha et al. 1991; Merritt & Sellwood 1994). When viewed edge-on the galaxies go from a disc-like shape to a much thicker peanut shape soon after the bar forms and become progressively rounder (Fig. 13). However, even after the central bulge-like structure has formed, the stellar/gaseous mass distribution remains visibly elongated even after several gigayears when seen face-on (Figs 10 and 12), which suggests that the bar has been significantly weakened but not completely destroyed. Its weakening is expected as a result of the growing central mass concentration (Hasan & Norman 1990; Friedli & Benz 1993; Norman, Sellwood & Hasan 1996). As the rotating bar evolves, stars also lose angular momentum to the surroundings and lead to an increased surface density. The increase in central density is more pronounced in

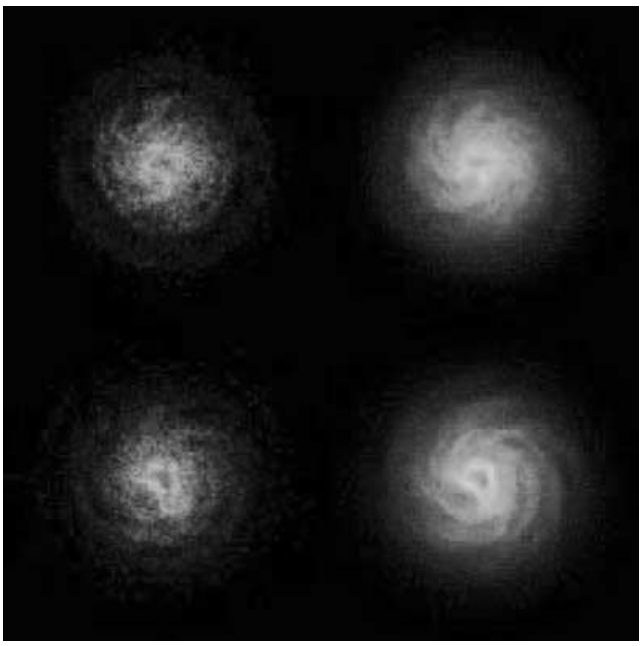

Figure 11. Grey-scaled face-on view of the disc density in model Lmd1c4sg (see Table 1). Brighter shades represent higher densities. Snapshots are taken after 3 Gyr (top) and 7 Gyr (bottom). The stellar distribution is shown on the left, the gas on the right. Boxes are 30 kpc on a side. This figure is available in colour in the on-line version of the journal on *Synergy*.

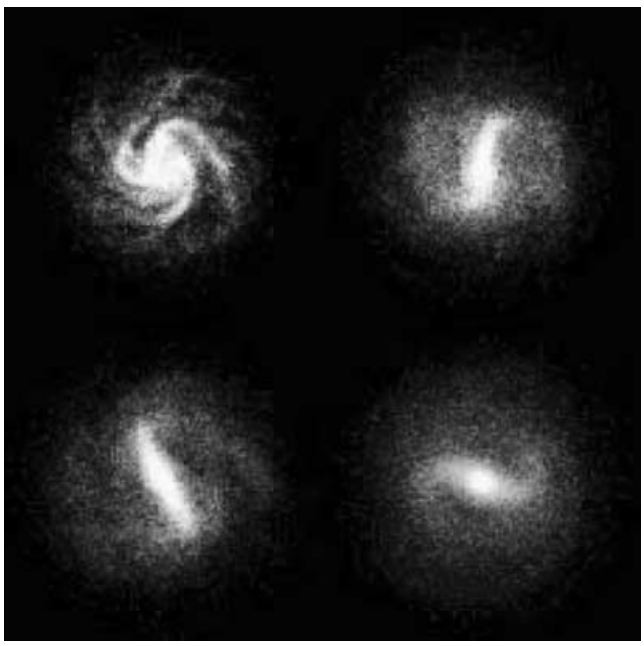

Figure 12. Grey-scaled face-on view of the stellar density of model Lmd2c12. Brighter shades represent higher densities. From the upper left to the bottom right, snapshots are shown at, respectively, 1, 3, 4.5 and 7 Gyr. Boxes are 25 kpc on a side. This figure is available in colour in the on-line version of the journal on *Synergy*.

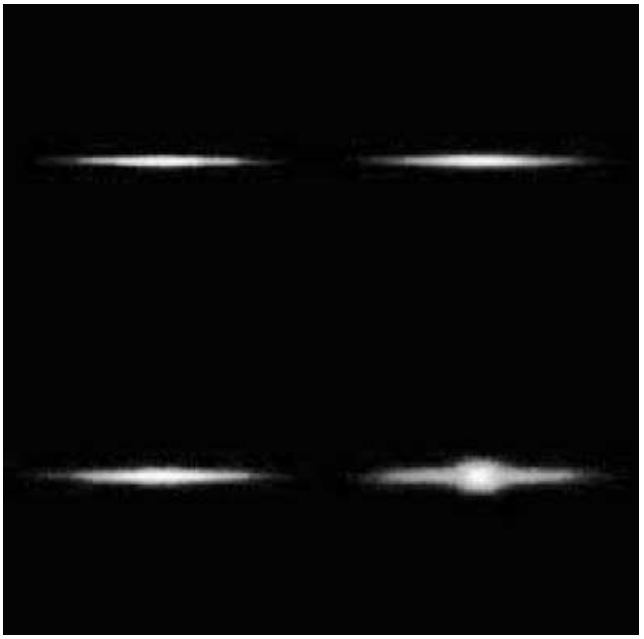

Figure 13. Grey-scaled edge-on view of the stellar density of model Lmd2c12. Brighter shades represent higher densities. From the upper left to the bottom right, snapshots are shown at, respectively, 1, 3, 4.5 and 7 Gyr. Boxes are 25 kpc on a side. This figure is available in colour in the on-line version of the journal on *Synergy*.

the gaseous disc (compare Figs 16 and 17). In fact, in addition to the gravitational losses already present in collisionless systems, some dissipation of angular momentum can occur in the shocks near the bar edges. In the adiabatic runs this is compensated by the subsequent heating and expansion of the gas, and in the end the inner profile looks more similar to that of the collisionless runs.

As a result of the increased central concentration of baryons, the latter become more dominant in the centre and change the shape of the galaxy's rotation curve. As shown in Figs 14 and 15, the way the shape varies can be different from case to case, but in general we observe that the peak velocity shifts inwards and often increases compared to the initial value (the more marked increase occurs in the gas dynamical runs). The central velocity dispersion increases by more than a factor of 2 during the morphological transformation, and hence the bulge-like structures are fairly hot systems ($v/\sigma \sim$ 0.6–0.7). However, the increase in the central density is really the most prominent feature, and it is the cause of the low Q parameters measured at the centre in the later stages (Figs 4 and 5). The evolving bars trigger a significant spiral pattern, particularly evident in the gas dynamical runs (Figs 9 and 10), which causes the galaxy to remain markedly non-axisymmetric even at large radii when the mass moments are measured (Fig. 7). An early-type spiral results, but one in which the disc has a very low surface density.

In what follows we will always identify the bulge with the inner, steeper part of the stellar density profile of the galaxies. Our definition is thus based on morphology and not on kinematics, although the component identified as the bulge is also kinematically distinct, having a v/σ a factor of 2 or more lower than the component that we identify as the disc. This central bulge has an exponential profile with a scalelength 5–10 times smaller than that of the surrounding disc (Figs 16–18). The disc is still exponential but considerably flatter than at the beginning; the scalelength always increases and can become more than twice as big in gas dynamical runs (Fig. 17);

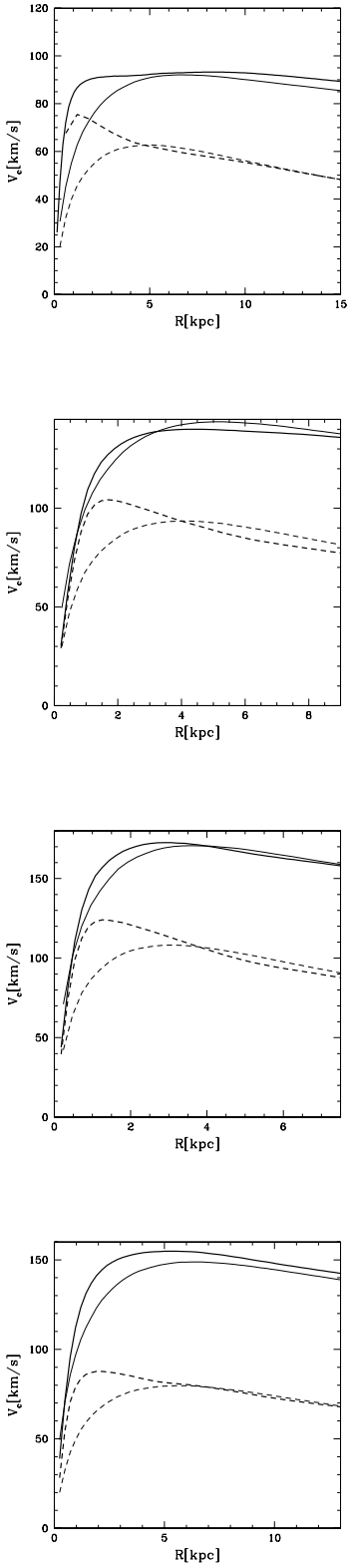

Figure 14. Evolution of the rotation curves of bar-unstable collisionless models. Thin lines are used for the initial curve, thick lines for the curve after 8 Gyr (solid for the total, dashed for stars only). Curves are shown out to four initial disc scalelengths. From top to bottom, models Lmd2c4, Lmd2c12, Lmd2c22 and Lmd2c22b are shown.

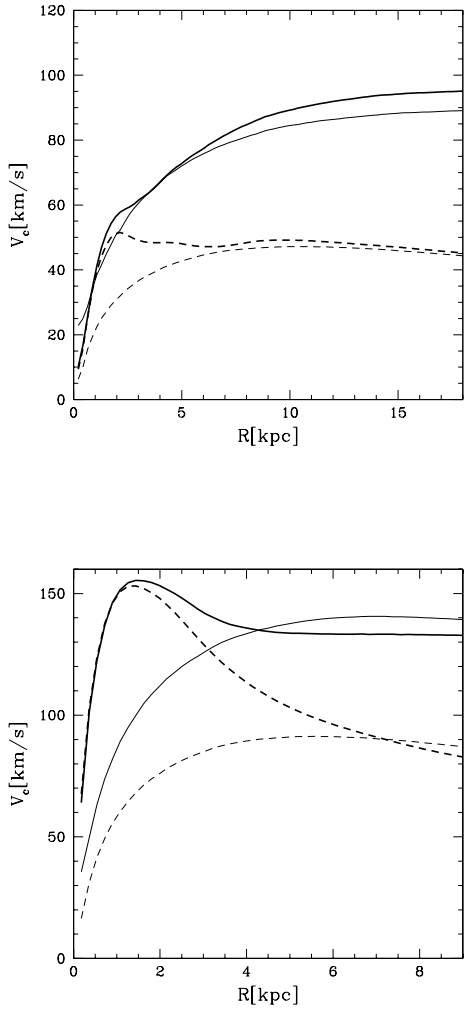

Figure 15. Evolution of the rotation curves of bar-unstable gas dynamical models. Thin lines are used for the initial curve, thick lines for the curve after 8 Gyr (solid for the total, dashed for stars only). Curves are shown out to four initial disc scalelengths. From top to bottom, models Lmd1c4 and Lmd2c12 (only isothermal runs) are shown.

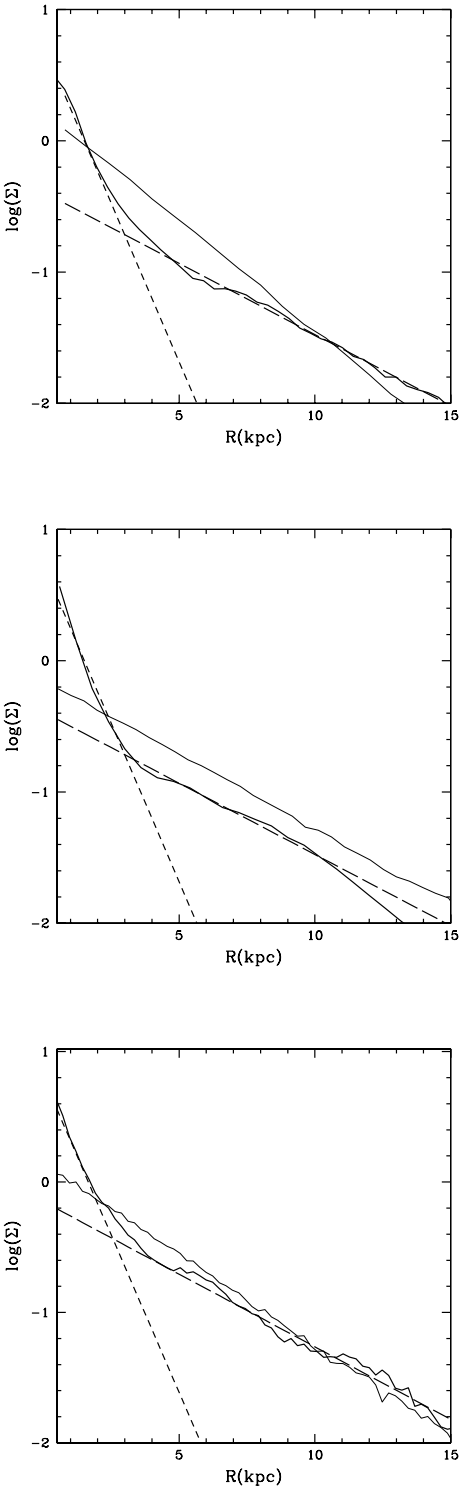

Figure 16. The final stellar surface density profile (thick solid line) is plotted along with the initial purely exponential profile (thin solid line). From top to bottom, models Lmd2c12, Lmd2c4 and Lmd2c22b are shown. Exponential fits to the inner (short-dashed line) and outer (long-dashed line) parts of the profile are shown, with scalelengths of, respectively, 900 pc, and 4, 4.2 and 3.9 kpc. The initial disc scalelengths were, respectively, 2.3, 3.6 and 3.3 kpc. The surface density is expressed in the units of the simulation.

the disc surface density also decreases, implying a disc central surface brightness a few magnitudes lower than in the initial conditions (Figs 16 and 17).

These and other properties of the final states of our bar-unstable models closely match those of the red early-type LSBGs studied by Beijersbergen et al. (1999). In the next section we will discuss in detail how far the comparison with such galaxies can be pushed.

Our simulations do not include star formation. We might ask how long a galaxy will remain in a mostly gaseous state as assumed for some of our models. Kennicutt (1998) and Martin & Kennicutt (2001) have shown that the Toomre Q parameter gives a good indication of the local density threshold above which star formation can occur. Observations of galaxies suggest that $Q < 1.44$ is required for star formation to proceed. Our gaseous discs satisfy the latter criterion nearly everywhere (except in the inner few hundred parsecs), but the star formation rates calculated from the local initial gas surface density as in Kennicutt (1998) would be as low as $\lesssim$0.3 $M_\odot$ yr^{-1} within 10 kpc (corresponding to a few disc scalelengths) for models with $f_d = 0.05$. Such modest star formation rates fall near the lowest measured by Kennicutt (1998) for spiral galaxies

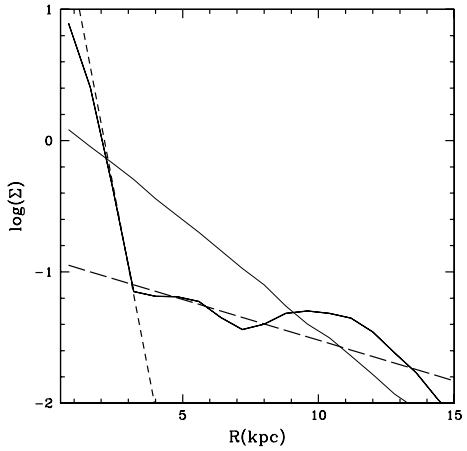

Figure 17. The final gas surface density profile (thick solid line) of model Lmd2c12g (see Table 1) is plotted along with the initial purely exponential profile (thin solid line). The results for the isothermal run are shown. Exponential fits to the inner (short-dashed line) and outer (long-dashed line) parts of the profile are shown, with scalelengths of, respectively, 800 pc and 9 kpc (while the initial disc scalelength was 2.3 kpc). The surface density is expressed in the units of the simulation.

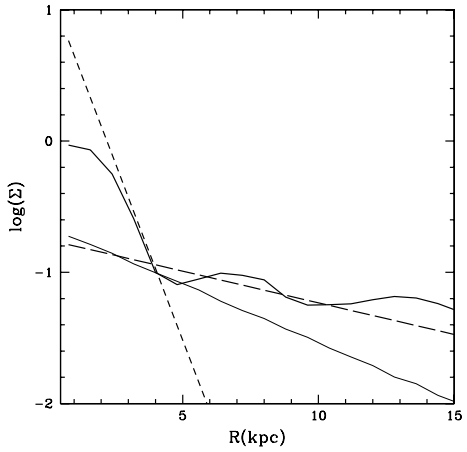

Figure 18. The final gas surface density profile (thick solid line) of model Lmd1c4g (see Table 1) is plotted along with the initial purely exponential profile (thin solid line). The results for the isothermal run are shown. Exponential fits to the inner (short-dashed line) and outer (long-dashed line) parts of the profile are shown, with scalelengths of, respectively, 400 pc and 7 kpc (while the initial disc scalelength was about 5 kpc). The surface density is expressed in the units of the simulation.

and are comparable to the star formation rates that Gerritsen & de Blok (1999) obtain in their simulations of LSBGs. The resulting gas consumption time-scale would exceed 25 Gyr for these model galaxies, and therefore these systems will remain mostly gaseous for most of their lifetime. In addition, these low star formation rates imply a weak supernovae feedback with little impact on the thermal and dynamical evolution of the gas, this being consistent with our assumption of an isothermal evolution. Of course, when significant non-axisymmetric structure, bars or clump-like features form, all these assumptions could break locally as the surface density grows above some threshold. In the light disc models ($f_{\rm d} = 0.05$) the surface density increases, on average, by only a factor of 2 in the bar region (in the inner few kiloparsecs in Fig. 17). Instead, in models with heavy discs the average surface density within 1–2 scalelengths increases by a factor of 10 (Fig. 18) and would result in a typical star formation rate of >20 $M_\odot$ yr^{-1} within 10 kpc, comparable to that of actively star-forming high surface brightness galaxies (Bell et al. 1999). The highest star formation rates would occur in the centre, inside the growing bulge-like component. As we mentioned, we believe that the final state of the heavy discs resembles the red LSBGs studied by Beijersbergen et al. (1999). Clearly, more quantitative predictions of the luminosity and colour evolution of the simulated galaxies demand that we include star formation and the mechanisms that can regulate it, for instance heating by ultraviolet radiation from hot stars and supernovae (Gerritsen & Icke 1997; Gerritsen & de Blok 1999). Simulations including these additional mechanisms will be the subject of a forthcoming paper. None the less, our main focus here is on the initial development of non-axisymmetric structure in both stellar and gaseous discs, and in this respect LSB models start with surface densities low enough to justify neglecting star formation and its effects.

4 DISCUSSION

We have shown that bar formation in low surface brightness stellar discs is unlikely unless they are more massive than usually believed. Light discs generate only transient non-axisymmetric distortions even when starting from a state with $Q < 1$. Instead, purely gaseous discs can become bar-unstable even for quite low masses provided that their haloes have low concentrations and their temperature stays low enough to maintain $Q \sim 1$ (as shown in the simulations adopting an isothermal equation of state). Growing modes are damped more easily in stellar discs because the velocity dispersion increases in response, raising Q to values well above unity; gaseous discs behave similarly only when the cooling is completely switched off (like in the experiments with an adiabatic equation of state). Although adopting an isothermal equation of state might seem simplistic, the temperatures we need to keep $Q \sim 1.2$ over most of the radial extent of our models, $T = 7500$ K, is typical of the H I component of spiral galaxies (Martin & Kennicutt 2001).

Concentrations for haloes forming at a redshift $\geqslant 2$ in LCDM models are sufficiently low ($c < 6$ at $V_{\rm c} < 80$ km s^{-1}) to include even the values required to drive bars in light gaseous discs (Bullock et al. 2001). The combination of a cold, mostly gaseous disc and a low-concentration halo was probably not uncommon at high redshift and perhaps so were barred LSBGs. However, when we look at the present-day distribution of halo concentrations in cosmological simulations (this is basically the combination of the distributions for objects formed at *any* redshift), we see that such low values are found for only a few per cent of the systems (Eke et al. 2001; Bullock et al. 2001).

On the other hand, massive discs contributing as much as 10 per cent to the total mass of the system become bar-unstable regardless of halo concentration, although the resulting bar tends to be longer (relative to the initial disc scalelength) in haloes with higher concentration (see Table 1). This is consistent with the findings of Athanassoula (2002) and Athanassoula & Mistriotis (2002), who claim that a higher halo mass within the disc region produces longer bars because these lose angular momentum more efficiently through resonant exchange with halo particles (but see also Athanassoula 2003).

As explained in Section 3.3, bars evolve into bulge-like structures in a few gigayears in both stellar and gas dynamical runs. The bulge reaches a surface density significantly higher than the rest of the disc (Figs 14–18). In models with gaseous bulges, a mean star formation rate ~ 1 $M_\odot$ yr^{-1} (inside the region characterized by the steeper

exponential, see Fig. 18) would result in light disc models following Kennicutt (1998) – this implies fairly rapid gas consumption timescales, $\lesssim$1 Gyr. In contrast, the rest of the disc will continue to form stars at a rate 10–20 times lower and will eventually keep a sufficient gas reservoir to form stars until the present epoch, thus maintaining rather blue colours like those of many observed LSBGs. Star formation rates 10–30 times higher would result in the bulges forming from massive discs; in this case a real starburst will likely convert most of the gas into stars in $\sim 10^8$ yr. In the latter case the bulge B-band surface brightness would be comparable to that of bulges of normal early-type spirals, $\mu_B \sim 19$ mag arcsec^{-2}, for a stellar mass-to-light ratio $\sim$1 (typical of a young stellar population) based on the stellar or gas surface density measured in our simulations. The bulge would eventually fade following the burst. Neglecting any further evolution of the surface density, if the stellar population undergoes passive evolution and reaches the typical stellar mass-to-light ratios of spheroids after a few gigayears, $(M/L_B)_* \sim 3$–4), the final central B-band surface brightness will be $\gtrsim$20 mag arcsec^{-2}. (These numbers are nearly independent of whether we consider the case of the models with only a stellar component or we compute surface densities from the models with gas assuming that this has been turned into stars.) Such systems would resemble the red LSBGs studied by Beijersbergen et al. (1999). The latter have a low surface brightness disc with central red bulges similar in structure to those of HSBGs but slightly fainter than them. Their bulge-to-disc ratios (B/D) in the I band (which should provide a good measure of the actual mass ratios) vary from less than 0.05 to as much as 0.5, and their total (disc plus bulge) B-band luminosity is $-21 < M_B < -17$. The final states of our models would have comparable luminosities, $-19.5 < M_B < -18.5$ [for $(M/L_B)_* = 2$] and the bulge contributes from 15 to 50 per cent of the total mass of the baryons (we measure the mass of the bulge as the mass contained within the radius at which the slope of the stellar profile steepens significantly). A meaningful comparison between our final states and the galaxies in Beijersbergen et al. (1999) should include their respective positions on the Tully–Fisher relation. Although kinematical data are not available for the observed galaxies, we can assume that they follow a B-band Tully–Fisher relation similar to that followed by other LSBGs (Zwaan et al. 1995). In that case their rotational velocities should be in the range 100–160 km s^{-1} for a luminosity $-19.5 < M_B < -18.5$ (the scatter in the measured velocities is indeed fairly large), which is consistent with the final peak velocities of our simulated galaxies (see Figs 14 and 15). A similar evolutionary scenario has been proposed recently by Noguchi (2001) to explain giant LSBGs which bear a resemblance to the red LSBGs but have a much larger size, bigger B/D ratios and even redder colours (Sprayberry et al. 1997).

However, while Noguchi starts from a model of a normal HSB galaxy (without gas), here we have shown that even galaxies that start with fairly low surface density discs can become bar-unstable and form a bulge provided that their disc is sufficiently massive with respect to the halo. The bulges that form in our models have both profiles and scalelengths that match those of the red, early-type LSBGs in Beijersbergen et al. (1999); they are fitted by exponential laws and their scalelengths are typically $\sim$0.1–0.2$R_{\rm h}$ (Figs 16–18). When translated into physical sizes, bulge scalelengths are as large as 0.4–0.9 kpc, i.e significantly larger than the bulges of 'normal' HSBGs of similar luminosity (de Jong & van der Kruit 1994). Being the product of secular disc evolution, the bulge scalelengths are correlated with those of the surrounding LSB discs, matching another feature of the galaxies in Beijersbergen et al. (1999) (for HSBGs a similar correlation is indeed found – see de Jong & van der Kruit 1994; MacArthur, Courteau & Holtzman 2003). Also, as already mentioned in Section 3.3, discs remain exponential but increase their scalelength by at least a factor of 2, reaching as much as 9 kpc (e.g. Fig. 17). Red early-type LSBGs also have discs with huge scalelengths, bigger than their blue counterparts for the same luminosity. Some of the red LSBGs also exhibit significant spiral structure; this appears to be triggered by the bar in our simulations and persists even after this has turned into a bulge, especially for purely gaseous discs (Figs 9 and 10).

In our scenario bulges form after a (gaseous) disc has already settled into the halo as a result of secular bar evolution. The bulge would be younger than the disc in a dynamical sense but after a few gigayears it would look redder than the latter due to the different mean age of its stars. Indeed, as we showed above, the different density structure of the two components suggests that, while an early burst of star formation is plausible for the bulge, the disc would undergo a weaker but more prolonged star formation. In particular, the spiral arms excited by the central bar would play an important role in the star formation history of the disc. Bars and rings are actually present in some of the red LSBGs, in which case they also have bluer colours in their central part. These systems resemble the intermediate stages seen in our simulations, while systems with distinct bulges are likely in the late evolutionary stage, and indeed they also look redder in the centre as if the stellar population there has already undergone significant fading. Future detailed observations of colour and age gradients throughout the disc and the bulge should enable better judgement of how realistic the scenario proposed here is. Simulations including star formation and explicit cooling and heating are better suited to explore this issue further and will be the subject of a forthcoming paper.

How large a population of LSBGs with bars/bulges should we expect based on our model? The naive expectation is that such galaxies should be rare as they originate from systems with disc mass fractions close to the upper limit for the baryon fraction (Jaffe et al. 2001). On the other hand, several authors, by modelling galaxy rotation curves, find a positive correlation between the spin parameter and the disc mass fraction (e.g. Van den Bosch, Burkert & Swaters 2001; Burkert 2003; Jimenez et al. 2003), which would imply that massive discs are more common among LSBGs. This correlation is not well understood. Burkert (2003) has proposed that it might result from a correlation between disc specific angular momentum (which might be different from that of the parent dark matter halo) and the disc mass fraction – however, at the moment it cannot be excluded that the correlation is produced by systematic errors in the procedure used to determine the dark halo parameters, especially when the rotation curves do not extend far enough in radius (Burkert, Van den Bosch & Swaters 2002; Verde et al. 2002). None the less, the recent analysis of 400 rotation curves reported in Jimenez et al. (2003) indicates that more than 50 per cent of high-spin systems (i.e. with $\lambda \geqslant 0.065$, the minimum value considered in this paper) have disc mass fractions near 0.1 (L. Verde, private communication). These results leave open the interesting possibility that many LSBGs are massive enough to become bar-unstable and undergo the morphological transformation described in this paper.

Relating the final state of bar-unstable but light ($f_{\rm d} < 0.1$) gaseous discs to known galaxies turns out to be less obvious. The bulge-like component that appears late in these systems would have an unusually low optical surface brightness as it forms out of gas having very low surface densities; assuming $(M/L_B)_* = 4$, as typical of old spheroid stellar populations, these bulges would have a B-band surface brightness $\sim$24 mag arcsec^{-2}. Such a low surface brightness is significantly lower than any of those of the objects studied in

Beijersbergen et al. (1999). However, although the bulge will be fainter than the disc and might be hardly recognizable in optical bands, it should still stand out when observed with longer wavelengths because of its intrinsically higher stellar density (see Figs 16–18). Many blue LSBGs or LSB dwarfs do not have significant spiral/non-axisymmetric structure, appearing rather amorphous or irregular (de Blok, Van der Hulst & Bothun 1995); on the basis of our results, the simplest interpretation of these systems is that they are stable because they have fairly light discs, $f_{\rm d} < 0.1$, and/or haloes as highly concentrated as expected in an LCDM model. Most of the galaxies whose measured rotation curves are nourishing the debate on dark matter cores would fall into the latter category. Therefore one would be tempted to conclude that bars cannot occur in these systems and hence cannot be invoked to explain the present-day structure of their inner halo. However, we cannot exclude that the available observations lack sufficient resolution and are still hiding some important clues to the past dynamical histories of these objects (see de Blok et al. 1999). New high-resolution observations of individual blue LSBGs at long wavelengths will show whether dim, red bulges are present in galaxies previously classified as blue, late-type LSBGs, and hence whether bar formation could have taken place in the past. Only if such spheroidal components turn out to be extremely rare will we conclude that bar formation, and thus bar/halo interactions, can be neglected for these galaxies. Interestingly, the recent observations in *J* and *K* bands by Galaz et al. (2002) suggest that at least a fraction of the systems that appear featureless in the optical hide a central red bulge or nucleus when observed in the near-infrared. Of course, high-resolution images might also reveal bar-like distortions. Indeed, some bars are observed in a few LSBGs included in a recent sample used by Swaters et al. (2003) to measure Hα rotation curves. These authors claim that the barred systems have slightly shallower halo inner slopes compared to the non-barred ones, although they admit that non-circular motions due to the bars themselves make the determination of the actual rotational velocity very hard and questionable in these cases.

However, even though evidence of present or past bars will be found in a number of LSBGs, our simulations do not provide strong support for a scenario in which bars can significantly affect the structure of the dark halo. In fact, the bars arising in our simulated galaxies are rather short, 3–8 times smaller than the halo scale radius, $r_{\rm s}$ (see Section 2), hence typically shorter than the long massive bars assumed in Weinberg & Katz (2002). (However, note that the bar in models Lmd2c12b and Lmd2c22b, which are the longest due to the large value of the spin parameter, approach the size of the bar considered in that paper relative to the halo scale radius.) Recent calculations by Sellwood (2003) show that, no matter how effective the transfer of angular momentum between the bar and the halo, bars up to four times smaller than $r_{\rm s}$ do not store enough angular momentum to produce the observed large dark matter cores. A particularly short bar arises in light discs (model Lmd1c4g), its size being >10 times smaller than $r_{\rm s}$, hence smaller than any of the bars studied by Sellwood (2003). Moreover, the fact that all the bars in our simulations, and especially the gaseous ones, seem to undergo a fast morphological evolution, casts some doubts about any significant dynamical impact on the dark halo. The large amount of mass transfer occurring during bar evolution, which tends to steepen the rotation curves, might cause the halo to contract in response, counteracting any eventual effect of the angular momentum exchange. The present simulations, although they have very high resolution by common standards, are not sophisticated enough to study the halo response in detail. In fact, whereas the inner halo profiles seem to change only marginally during the evolution, we have noticed that the amount of change depends on the choice of the gravitational softening (in general, the smaller the softening, the steeper is the final halo profile). A higher mass resolution is required to allow the use of smaller softenings, and very likely it is also necessary to resolve adequately the spectrum of resonances between halo and star particles (Weinberg & Katz 2002). Therefore we decided to postpone the analysis of the bar–halo interaction to a forthcoming paper, in which we will use a mass resolution up to 10 times higher than that adopted here, and a correspondingly higher force resolution.

5 SUMMARY

In this paper we have shown that bar formation in LSBGs is possible, yet the initial conditions required for this to happen apply to only a narrow region of the parameter space made available by currently favoured hierarchical models of structure formation. In addition, the characteristics of the bars that eventually form in such systems as well as their rapid morphological evolution hardly support the idea that bar–halo interactions play a crucial role in shaping the inner structure of the dark matter halo. Our main findings are summarized as follows:

(i) The halo/disc mass ratio within the region where the disc lies determines whether the LSB models studied are stable or not. This ratio is fixed once both the halo concentration and the disc mass are fixed and sets the degree of swing amplification of $m = 2$ modes. In particular, LSBGs with discs as massive as 10 per cent of the halo mass can become bar-unstable for a wide range of concentrations, including the highest values expected in LCDM models.

(ii) LSBGs with (typical) light discs ($f_{\rm d} < 0.1$) can become bar-unstable if their halo concentration is as low as $c = 4$ and their discs are essentially gaseous and cold. Such low concentrations are rare among LCDM haloes.

(iii) Bars forming in LSBGs are significantly shorter than the halo scale radius. They are not expected to have a large enough reservoir of orbital angular momentum to effectively change the inner density profile of dark matter haloes and turn the cusp into a core.

(iv) Both gaseous and stellar bars evolve into central bulge-like structures after a few gigayears. The bar and the bulge have surface densities up to two orders of magnitude higher than the surrounding low surface density discs. Radically different star formation histories are thus expected in the central part of the galaxy as opposed to the extended disc.

(v) The structural properties of the final states (after up to 10 Gyr of evolution) of bar-unstable, massive LSB discs are consistent with those of the red, early-type LSBGs observed by Beijersbergen et al. (1999). Our secular evolution scenario naturally explains observed correlations like that between the disc and bulge scalelengths.

(vi) Blue LSBGs included in samples used to measure rotation curves usually appear featureless in the optical. Our findings imply that a dim, red bulge-like component must be present at their centre if they ever formed a bar. Future observations of these galaxies in the near-infrared should reveal whether these hidden bulges exist in most LSBGs. First attempts in this direction (Galaz et al. 2002) suggest that this might be the case.

ACKNOWLEDGMENTS

LM is grateful to Victor Debattista for carefully reading an early version of the paper and for providing plenty of useful comments and suggestions, and to the anonymous referee for providing an insightful review that considerably improved the paper. We also

thank James Schombert, Martin Weinberg, Neal Katz and Thomas Quinn for interesting and stimulating discussions on LSBGs and on the dynamics of barred galaxies, and Julianne Dalcanton and Licia Verde for helpful information on recent observational data. The simulations were performed on the 64-processor Intel cluster at the University of Washington, on the Compaq-Alpha cluster (LeMieux) at the Pittsburgh Supercomputing Center, and on the ORIGIN 3800 at CINECA.

REFERENCES

Athanassoula E., 2002, ApJ, 569, L83
Athanassoula E., 2003, MNRAS, 341, 1117
Athanassoula E., Mistriotis A., 2002, MNRAS, 330, 35
Athanassoula E., Sellwood J. A., 1986, MNRAS, 221, 213
Balsara D. S., 1995, J. Comput. Phys., 121, 357
Barnes E. I., Tohline J. E., 2001, ApJ, 550, 884
Beijersbergen M., de Blok W. J. G., Van der Hulst J. M., 1999, A&A, 351, 903
Bell E. F., Bower R. G., de Jong R. S., Hereld M., Rauscher B. J., 1999, MNRAS, 302, L55
Benson A. J., Bower R. G., Frenk C. S., Lacey C. G., Baugh C. M., Cole S., 2003, ApJ, submitted (astro-ph/0302450)
Bergmann M. P., Jorgensen I., Hill G., 2003, AJ, 125, 116
Binney J., Tremaine S., 1987, Galactic Dynamics. Princeton Univ. Press, Princeton, NJ
Bothun G. D., Impey C., Malin D., 1986, BAAS, 18, 958
Bothun G. D., Impey C. D., Malin D. F., Mould J. R., 1987, AJ, 94, 23
Bothun G. D., Schombert J. M., Impey C. D., Sprayberry D., McGaugh S., 1993, AJ, 106, 530
Bullock J. S., Kolatt T. S., Sigad Y., Somerville R. S., Kravtsov A. V., Klypin A. A., Primack J. R., Dekel A., 2001, MNRAS, 321, 559
Burkert A., 2003, Ap&SS, 284, 697
Burkert A., Van den Bosch F., Swaters R. A., 2002, preprint (astro-ph/0202024)
Carollo C. M., Stiavelli M., de Zeeuw P. T., Seigar M., Dejonghe H., 2001, ApJ, 546, 216
Cazes J. E., Tohline J. E., 2000, ApJ, 532, 1051
Christodoulou D. M., Shlosman I., Tohline J. E., 1995, ApJ, 443, 551
Chung A., van Gorkom J. H., O'Neil K., 2002, AJ, 123, 2387
Colpi M., Mayer L., Governato F., 1999, ApJ, 525, 720
Combes F., Sanders R. H., 1981, A&A, 96, 161
Combes F., Debbasch F., Friedli D., Pfenniger D., 1990, A&A, 233, 82
Dalcanton J. J., Spergel D. N., Summers F. J., 1997, ApJ, 482, 659
Debattista V. P., Sellwood J. A., 1998, ApJ, 493, L5
Debattista V. P., Sellwood J. A., 2000, ApJ, 543, 704
de Blok W. J. G., Bosma A., 2002, A&A, 385, 816
de Blok W. J. G., McGaugh S. S., 1997, MNRAS, 290, 533
de Blok W. J. G., Van der Hulst J. M., 1998a, A&A, 335, 421
de Blok W. J. G., Van der Hulst J. M., 1998b, A&A, 336, 49
de Blok W. J. G., Van der Hulst J. M., Bothun G. D., 1995, MNRAS, 274, 235
de Blok W. J. G., McGaugh S. S., Van der Hulst T., 1996, MNRAS, 283, 18
de Blok E., Walter F., Bell E., 1999, A&A, 269, 101
de Blok W. J. G., McGaugh S. S., Rubin V. C., 2001a, A&A, 122, 2381
de Blok W. J. G., McGaugh S. S., Rubin V. C., 2001b, A&A, 122, 2396
de Blok W. J. G., McGaugh S. S., Bosma A., Rubin V. C., 2001c, ApJ, 552, L23
Dehnen W., 2001, MNRAS, 324, 273
de Jong R. S., van der Kruit P. C. , 1994, A&AS, 106, 451
Efstathiou G., Lake G., Negroponte J., 1982, MNRAS, 199, 1069
Eke V. R., Navarro J. F., Steinmetz M., 2001, ApJ, 554, 114
Elmegreen B., 1995, MNRAS, 275, 944
Eskridge et al., 2000, AJ, 119, 536
Fall S. M., Efstathiou G., 1980, MNRAS, 193, 189
Flores R. A., Primack J. R., 1994, ApJ, 472, L1
Friedli D., Benz W., 1993, A&A, 268, 65
Friedli D., Benz W., 1995, A&A, 301, 649
Fukugita M., Hogan C. J., Peebles P. J. E., 1998, ApJ, 503, 518
Galaz G., Dalcanton J., Infante L., Treister E., 2002, AJ, 124, 1360
Gardner J. P., 2001, ApJ, 557, 616
Gerin M., Combes F., Athanassoula E., 1990, A&A, 230, 37
Gerritsen J. P. E., de Blok W. J. G., 1999, A&A, 342, 655
Gerritsen J. P. E., Icke V., 1997, A&A, 325, 972
Governato F. et al., 2002, ApJ, submitted (astro-ph/0207044)
Hasan H., Norman C., 1990, ApJ, 361, 69
Hernandez X., Gilmore G., 1998, MNRAS, 291, 595
Hernquist L., 1993, ApJS, 86, 289
Hernquist L., Katz N., 1989, ApJS, 70, 419
Hernquist L., Weinberg M. D., 1992, MNRAS, 400, 800
Hernquist L., Hut P., Makino J., 1993, ApJ, 402, L85
Impey C. D., Sprayberry D., Irwin M. J., Bothun G. D., 1996, ApJS, 105, 209
Jaffe A. H. et al., 2001, Phys. Rev. Lett., 86, 3475
Jimenez R., Padoan P., Matteucci F., Heavens A. F., 1998, MNRAS, 229, 123
Jimenez R., Verde L., Peng Oh S., 2003, MNRAS, 339, 243
Jog C. J., 1992, ApJ, 390, 378
Jog C. J., 1996, MNRAS, 278, 209
Katz N., Gunn J. E., 1991, ApJ, 377, 365
Katz N., Hernquist L., Weinberg D. H., 1992, ApJ, 399, L109
Kennicutt R. C. Jr, 1998, ApJ, 498, 541
Laurikainen E., Salo H., 2002, MNRAS, 337, 1118
Laurikainen E., Salo H., Rautiainen P., 2002, MNRAS, 331, 880
Lemson G., Kauffmann G., 1999, MNRAS, 302, 111
MacArthur L. A., Courteau S., Holtzman J. A., 2003, ApJ, 582, 689
McGaugh S. S., Schombert J. M., Bothun G. D., de Blok W. J. G., 2000, ApJ, 533, L99
MacLow M. M., Ferrara A., 1999, ApJ, 513, 142
Martin C. L., 1999, ApJ, 513, 156
Martin C. L., Kennicutt R. C. Jr, 2001, ApJ, 555, 258
Martin P., 1995, AJ, 109, 2428
Mayer L., Governato F., Colpi M., Moore B., Quinn T., Wadsley J., Stadel J., Lake G., 2001a, ApJ, 547, L123
Mayer L., Governato F., Colpi M., Moore B., Quinn T., Wadsley J., Stadel J., Lake G., 2001b, ApJ, 559, 754
Mayer L., Moore B., Quinn T., Governato F., Stadel J., 2002, MNRAS, 336, 119
Merritt D., Sellwood J. A., 1994, ApJ, 425, 530
Mihos J. C., McGaugh S. S., de Blok W. J. G., 1997, ApJ, 477, L79
Mo H. J., Mao S., White S. D. M., 1998, MNRAS, 296, 847
Moore B., Katz N., Lake G., 1996, ApJ, 457, 455
Moore B., Lake G., Quinn T., Stadel J., 1999a, MNRAS, 304, 465
Moore B., Quinn T., Governato F., Stadel J., Lake G., 1999b, MNRAS, 310, 1147
Moore N., 1994, Nat, 370, 629
Navarro J., Steinmetz M., 2000, ApJ, 538, 477
Navarro J. F., Frenk C. S., White S. D. M., 1995, MNRAS, 275, 56
Navarro J., Eke V., Frenk C., 1996, MNRAS, 283, L72
Navarro J. F., Frenk C. S., White S. D. M., 1997, MNRAS, 290, 493
Noguchi M., 2001, MNRAS, 328, 353
Norman C., Sellwood J. A., Hasan H., 1996, ApJ, 462, 114
O'Neil K., Bothun G. D., Schombert J., 1998, AJ, 116, 2776
O'Neil K., Bothun G. D., Schombert J., 2000, AJ, 119, 1360
Pfenniger D., 1984, A&A, 134, 373
Pfenniger D., 1985, A&A, 150, 97
Raha N., Sellwood J. A., James R. A., Kahn F. D., 1991, Nat, 352, 411
Regan M. W., Elmegreen D. M., 1997, AJ, 114, 965
Romeo A. B., 1992, MNRAS, 256, 307
Romeo A. B., 1994, A&A, 799, 806
Schombert J., Bothun G., Schneider S., McGaugh S., 1992, AJ, 103, 107
Schombert J. M., McGaugh S. S., Eder J. A., 2001, AJ, 121, 2420
Sellwood J. A., 2003, ApJ, 587, 638
Sellwood J. A., Evans N. W., 2001, ApJ, 546, 176
Sellwood J. A., Moore E. M., 1999, ApJ, 510, 125

Sommer-Larsen T. J., Gotz M., Portinari L., 2002, Ap&SS, 281, 519
Spergel D. N. et al., 2003, ApJS, 148, 175
Sprayberry D., Impey C. D., Irwin M. J., Bothun G. D., 1997, ApJ, 482, 104
Springel V., Hernquist L., 2003, MNRAS, 339, 289
Springel V., White S. D. M., 1999, MNRAS, 307, 162
Stadel J., 2001, PhD thesis
Stadel J., Wadsley J., Richardson D. C., 2002, in Dimopoulos N. J., Lie K. F., eds, High Performance Computing Systems and Applications. Kluwer Academic, Boston, p. 501
Swaters R. A., Madore B. F., Trewhella M., 2000, ApJ, 531, L107
Swaters R. A., Madore B. F., Van den Bosch F. C., Balcells M., 2003, ApJ, 583, 732s
Taffoni G., Mayer L., Colpi M., Governato F., 2003, MNRAS, 341, 434
Thacker R. J., Couchman H. M. P., 2001, ApJ, 555, L17
Toomre A., 1964, ApJ, 139, 1217
Toomre A., 1981, in Fall S. M., Lynden-Bell D., eds, The Structure and Evolution of Normal Galaxies. Cambridge Univ. Press, Cambridge, p. 111
Valenzuela O., Klypin A., 2003, MNRAS, 345, 406
Van den Bosch F. C., Swaters R. A., 2001, MNRAS, 325, 101
Van den Bosch F. C., Robertson B. E., Dalcanton J. J., de Blok W. J. G., 2000, AJ, 119, 1579
Van den Bosch F. C., Burkert A., Swaters R. A., 2001, MNRAS, 326, 1205
Van den Hoek L. B., de Blok W. J. G., Van der Hulst J. M., de Jong T., 2000, A&A, 357, 397
Velazquez H., White S. D. M., 1999, MNRAS, 304, 254
Verde L., Peng Oh S., Jimenez R., 2002, MNRAS, 336, 541
Verheijen M., de Blok E., 1999, Ap&SS, 269, 673
Wadsley J., Stadel J., Quinn T., 2003, New Astron., submitted
Weinberg M. D., 2000, ApJ, 532, 922
Weinberg M. D., Katz N., 2002, ApJ, 580, 627
Zwaan M. A., Van der Hulst J. M., de Blok W. J. G., McGaugh S. S., 1995, MNRAS, 273, L35

This paper has been typeset from a TEX/LATEX file prepared by the author.